

VIP Special Collection

Reactivity of a Strictly T-Shaped Phosphine Ligated by an Acridane Derived NNN Pincer Ligand

Aaron J. King,^[a] Josh Abbenseth,^{*,[a, b]} and Jose M. Goicoechea^{*,[c]}

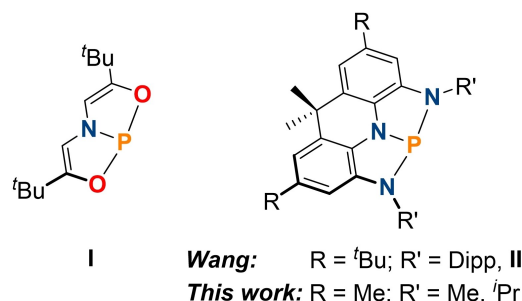
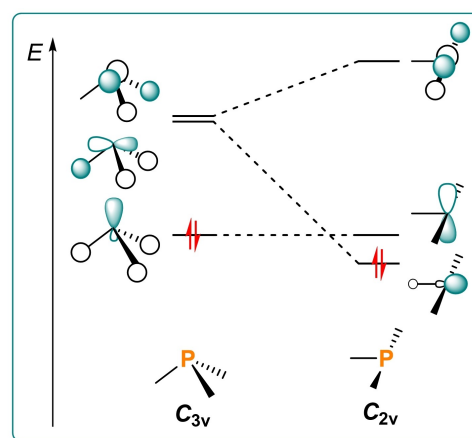
Abstract: The steric tuning of a tridentate acridane-derived NNN pincer ligand allows for the isolation of a strictly T-shaped phosphine that exhibits ambiphilic reactivity. Well-defined phosphorus-centered reactivity towards nucleophiles and electrophiles is reported, contrasting with prior reports on this class of compounds. Reactions towards oxidants are also described. The latter result in the two-electron oxidation of the phosphorus atom from +III to +V and are accom-

panied by a strong geometric distortion of the NNN pincer ligand. By contrast, cooperative activation of E–H (HCl, HBcat, HOME) bonds proceeds with retention of the phosphorus redox state. When using H₂O as a substrate, the reaction results in the full disassembly of H₂O to its constituent atoms, highlighting the potential of this platform for small molecule activation reactions.

Introduction

The ability of certain main group elements to mimic reactivity inherently associated with transition metals has recently become a concept of significant interest.^[1–5] Amongst the elements of the p-block, phosphorus has emerged as a highly viable candidate for such a purpose due to its accessible phosphorus(III/V) redox couple, which facilitates the required electron transfer processes for oxidative-addition and reductive-elimination reactions.^[6–9] Judicious choice of a co-ligand can be used to facilitate cooperative substrate activation as well.^[10] While phosphines predominantly exhibit nucleophilic reactivity, the incorporation of phosphorus into tridentate pincer ligands enforces a non-VSEPR symmetry, and permits phosphorus-based ambiphilic behavior. This is a consequence of lifting the degeneracy of the σ -antibonding LUMOs (lowest unoccupied molecular orbitals) found in trigonal phosphines, resulting in a

reduced HOMO-LUMO separation that enables electron donor *and* acceptor properties at phosphorus. Full perturbation towards a T-shape (or C_{2v} symmetry) results in a frontier-orbital arrangement that is highly reminiscent of those found in tetrylenes, albeit with a significantly reduced directionality of the s-type lone pair situated at the phosphorus center (Figure 1, top).^[11–14] Several geometrically constrained phosphines (and



[a] A. J. King, Dr. J. Abbenseth
Department of Chemistry
University of Oxford,
Chemistry Research Laboratory
12 Mansfield Road, Oxford, OX1 3TA (UK)

[b] Dr. J. Abbenseth
Institut für Chemie
Humboldt-Universität zu Berlin
Brook-Taylor-Straße 2, 12489 Berlin (Germany)
E-mail: josh.abbenseth@hu-berlin.de

[c] Prof. J. M. Goicoechea
Department of Chemistry
Indiana University
800 E. Kirkland Ave., Bloomington, In, 47401 (USA)
E-mail: jgoicoec@iu.edu

Supporting information for this article is available on the WWW under <https://doi.org/10.1002/chem.202300818>

Part of a Special Collection on the p-block elements.

© 2023 The Authors. Chemistry - A European Journal published by Wiley-VCH GmbH. This is an open access article under the terms of the Creative Commons Attribution License, which permits use, distribution and reproduction in any medium, provided the original work is properly cited.

Figure 1. The effect of changing the geometry of a phosphine from C_{3v} towards C_{2v}, upon geometric constraint (top); C_{2v} symmetric geometrically constrained phosphines reported in the literature (bottom). Dipp = 2,6-diisopropylphenyl.

phosphenium cations, i.e. PR_2^+ species) with ONO ,^[15–29] OON ,^[30] CCC ,^[31–33] NNN ,^[34–49] NPN ,^[50,51] SPS ,^[52–54] or NNS ^[55] donor sets have been reported, each showing unusual reactivity towards small molecules and unique spectroscopic and electronic properties.^[37]

Due to the lack of rigidity of many of these reported pincer ligands, these species adopt a *bent* geometry. However, on account of the reduced HOMO-LUMO gap, electrophilic substrate activation is most efficient at the *planar* T-shaped conformer. Consequently, kinetic barriers for bond activation reactions are influenced by the required geometric distortion to access this more reactive state, impairing the activity of systems that cannot fully distort to a C_{2v} geometry. The strictly T-shaped phosphine I (Figure 1, bottom), initially reported by the Arduengo group, and further investigated by Driess, Radosevich and co-workers, has been shown to react with a plethora of small molecules.^[18,25,36] To date, this is still the only strictly T-shaped phosphine for which reactivity studies have been reported. The bis-enolate ligand in I, however, proved to be highly reactive, especially towards protic E–H bonds, and was shown to participate in substrate activation reactions resulting in ligand derivatization or complete disassembly of the ligand scaffold.^[24,25,29,36] The redox chemistry of the acridane derived T-shaped phosphine II was recently investigated by Wang and co-workers (Figure 1, bottom).^[46] Although further chemistry was not reported, this system holds immense potential for phosphorus-based reactivity and possible redox activity due to the increased chemical inertness and high rigidity of the ligand backbone.^[56–58] In addition, extensive computational studies by Zhu, Zeng, Maeda, Sakaki and co-workers have suggested that phosphines ligated by NNN donor sets, in particular acridane derived systems, could be highly active in small molecule activation reactions, for example catalytic CO_2 reduction to formic acid,^[59] ammonia-borane dehydrogenation,^[60] and even dinitrogen splitting.^[61]

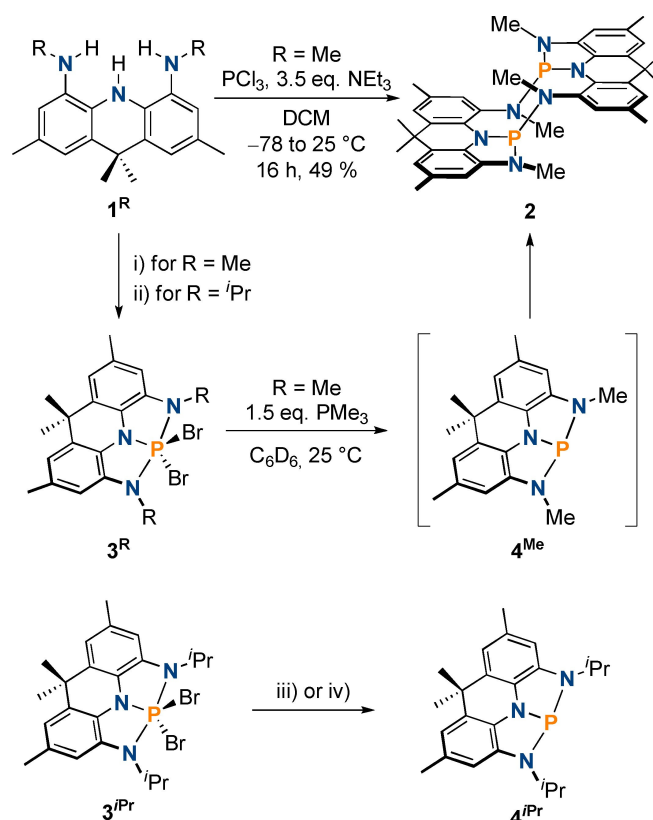
We recently reported the synthesis of NNN pincer ligand 1^{Pr} (Scheme 1) and its use in the synthesis of tantalum(V) complexes for the activation of small molecule substrates.^[62] The scalable synthesis and the possibility of easily varying the flanking nitrogen donors of this pincer scaffold motivated us to prepare strictly T-shaped phosphines based on this ligand framework. The work described herein aims to realize the phosphorus centered ambiphilic reactivity patterns predicted for such systems and evaluate their performance in small molecule activation reactions.

Results and Discussion

Synthesis of NNN ligated phosphines and phosphoranes

We synthesized the trisamine 1^{Me} in a multi-step procedure, starting from 2,7,9,9-tetramethyl-9,10-dihydroacridine in 79% isolated yield.^[63]

Incorporation of phosphorus was attempted by reacting 1^{Me} with PCl_3 in the presence of NEt_3 (Scheme 1). The $^{31}\text{P}\{^1\text{H}\}$ NMR spectrum of the reaction mixture reveals the formation of a



Scheme 1. Reactivity of the protio-ligand 1^{R} towards PCl_3 and PBr_5 in the presence of NEt_3 to generate 2 and 3^{R} as well as conversion of 3^{Me} towards 2 via transient 4^{Me} (top); Generation of 4^{IPr} from 3^{IPr} upon dehalogenation with PMe_3 or Mg (bottom); i) PBr_5 , 3 equiv. NEt_3 , toluene, -78 to 25 °C, 16 h, 64% isolated yield; ii) PBr_5 , 5 equiv. NEt_3 , toluene, -78 to 25 °C, 16 h, 54% isolated yield; iii) 5 equiv. PMe_3 , C_6H_6 , 25 °C, 15 min, 90% isolated yield; iv) 20 equiv. Mg , THF , 25 °C, 30 min, 90% isolated yield.

major product at 112.1 ppm (49% isolated yield). However, the ^1H NMR spectrum shows that the formed product is not C_{2v} symmetric as would be expected for the targeted T-shaped phosphine, but rather that it exhibits C_1 symmetry on the NMR timescale. Single crystal X-ray diffraction (SXRD) shows that the bisphosphine 2 was instead formed (Figure 2), which supports the recorded ^1H NMR spectrum. 2 features a central 10-membered ring linking both acridane fragments. The SXRD structure is consistent with retention of the phosphorus(III) redox state over the course of the reaction, in line with NMR spectroscopic analysis. 2 is likely formed by dimerization of a transient highly electrophilic T-shaped phosphine, akin to reports by Chitnis, Wolf and co-workers for NNN ligated antimony and bismuth pincer compounds and ONO ligated phosphines, respectively.^[16,64]

To further substantiate this claim, we aimed to access the targeted species via reduction of an NNN ligated phosphorus(V) precursor. The dibromo-phosphorane 3^{Me} can be accessed by reaction of the protio-ligand 1^{Me} with PBr_5 in the presence of NEt_3 (Scheme 1, 64% isolated yield). 3^{Me} is C_{2v} symmetric on the NMR timescale and features a phosphorus chemical shift of -107.6 ppm. This compares well with other recently reported

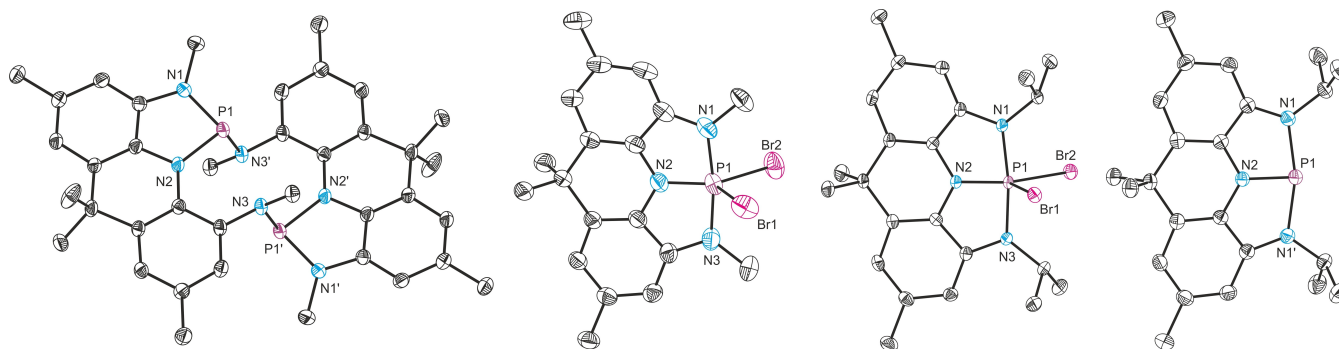


Figure 2. From left to right: single crystal X-ray structures of **2**, **3^{Me}**, **3^{iPr}** and **4^{iPr}**. Thermal ellipsoids pictured at 50% probability level. Hydrogen atoms and solvent of crystallization removed for clarity.

dibromophosphoranes bearing pincer-type ligands and is within the chemical shift region expected for a phosphorus(V) species.^[21] The P–N bond distances (1.653(2) and 1.768(2) Å) derived by single crystal X-ray diffraction are in line with the formation of single bonds, suggesting no oxidation of the redox non-innocent ligand framework (Figure 2).

When **3^{Me}** is reacted with 1.5 equiv. PMe_3 in benzene, a bright orange solution is generated and PMe_3Br_2 immediately precipitates out of the reaction mixture due to phosphine-mediated dehalogenation of **3^{Me}**.^[65–69] A new resonance at 150.9 ppm is observed in the $^{31}\text{P}\{^1\text{H}\}$ NMR spectrum (Figure S59). This chemical shift (and color, see below) are as expected for geometrically constrained phosphines, allowing the tentative assignment of this species as T-shaped phosphine **4^{Me}** (Scheme 1). However, over the course of minutes the solution turns yellow and the aforementioned $^{31}\text{P}\{^1\text{H}\}$ NMR signal converts to that of diphosphine **2**.

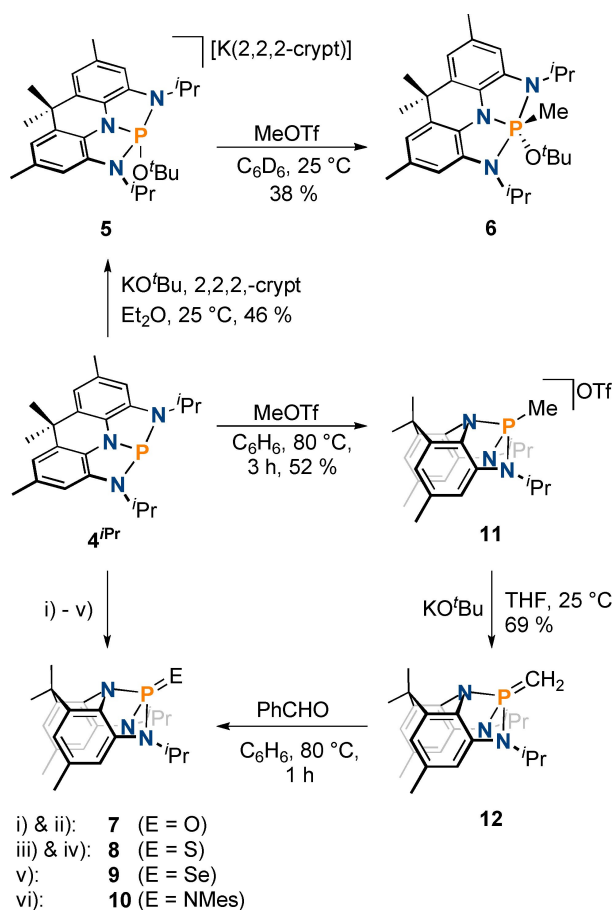
The crystal structure of **2** suggests that a slight increase in the steric bulk of the flanking nitrogen substituents might be sufficient to stabilize a monomeric T-shaped phosphine. Therefore, the previously reported trisamine **1^{iPr}** (which possesses bulkier isopropyl substituents) was employed. However, reaction of **1^{iPr}** with PCl_3 in the presence of NEt_3 resulted in the formation of numerous species as observed by $^{31}\text{P}\{^1\text{H}\}$ NMR spectroscopy (Figure S61). As a clean and direct synthesis of **4^{iPr}** was not possible from PCl_3 , we sought to access a phosphorus(V) species which can, in turn, be reduced to the phosphine. Dibromophosphorane **3^{iPr}** could be accessed in 54% isolated yield upon reaction of **1^{iPr}** with PBr_5 and NEt_3 (Scheme 1). The molecular structure of **3^{iPr}** as determined by SXRD and ^1H and $^{31}\text{P}\{^1\text{H}\}$ NMR spectroscopy closely resemble the data obtained for **3^{Me}** (Figure 2). In stark contrast to the reactivity of **3^{Me}** upon dehalogenation, treatment of **3^{iPr}** with PMe_3 or Mg powder results in the clean formation of the phosphine **4^{iPr}** (90% isolated yield) which exhibits increased stability in solution when compared to its smaller congener **4^{Me}** (Scheme 1); after several days only traces of additional signals appear in the $^{31}\text{P}\{^1\text{H}\}$ NMR spectrum (< 5%, Figure S63). The $^{31}\text{P}\{^1\text{H}\}$ chemical shift (150.0 ppm) and the overall C_{2v} symmetry on the NMR timescale, as observed by ^1H NMR spectroscopy, corroborate formation of a T-shaped phosphine.^[29,46] The

molecular structure of **4^{iPr}** derived by SXRD reveals strict planarity and a buried volume of $\%V_{\text{bur}}=63\%$ around the phosphorus center (angle sum of 360° , Figure 2).^[70] Furthermore, the contraction of the C–N bond lengths when compared to **3^{iPr}** indicate partial electromorphism stemming from the redox non-innocent nature of the NNN pincer scaffold.^[34,46]

Ambiphilic reactivity and two-electron oxidation reactions

The non-VSEPR structure of pincer type phosphines affords a low-lying empty p-type orbital situated on the phosphorus atom, enabling electrophilic reactivity.^[7] We aimed to address this property by formation of the anionic phosphorus alkoxide **5** upon reaction of **4^{iPr}** with KO^tBu in the presence of 4,7,13,16,21,24-hexaoxa-1,10-diazabicyclo[8.8.8]hexacosan (2,2,2-crypt; Scheme 2, 46% isolated yield). A low-resolution single crystal X-ray diffraction structure reveals that the planarity of the pincer ligand is maintained on coordination of the alkoxide to the phosphorus center (Figure S74). Unfortunately, the low quality of the crystals prevents a meaningful discussion of bond metric parameters. The $^{31}\text{P}\{^1\text{H}\}$ chemical shift of 50.0 ppm compares well with related anionic phosphorus alkoxides.^[20] We were interested if subsequent treatment with the strong electrophile MeOTf would result in phosphorus-centered reactivity or functionalization of the ligand periphery as demonstrated by Aldridge, Goicoechea and co-workers.^[20] Addition of MeOTf to **5** results in the instant formation of a new resonance at -39.4 ppm in the $^{31}\text{P}\{^1\text{H}\}$ NMR spectrum, indicative of phosphorus oxidation to phosphorus(V), reminiscent of recently described nucleophilic reactivity of a geometrically constrained phosphoranide.^[71] ^1H NMR spectroscopy and SXRD further confirm that the C_s symmetric phosphorane **6** was formed (Scheme 2, Figure 3, 38% isolated yield). NMR spectroscopic analysis of the reaction mixture gave no indications of competing methylation of the adjacent nitrogen atoms in stark contrast to previous findings.^[20,51]

An established reactivity pattern of transition metals towards chalcogens consists of formation of $\text{M}=\text{E}$ double bonds accompanied by two electron oxidation of the metal center. This type of reactivity is surprisingly rare for phosphorus pincer



Scheme 2. Electrophilic functionalization of 4^{iPr} to give **5** and subsequent methylation yielding **6**; Generation of phosphorus(V) chalcogenides **7–9**; nucleophilic reactivity of 4^{iPr} towards methyl triflate to yield **10**, its subsequent deprotonation to form **11**, and its conversion to **7**; i) xs. O_2 , THF, $60^\circ C$, 16 h, 55%; ii) 1 equiv. pyridine N-oxide, C_6D_6 , $25^\circ C$, 16 h, 57% isolated yield; iii) 5 equiv. S_8 , CD_2Cl_2 , $25^\circ C$, 4 h, observed spectroscopically; iv) 1 equiv. Lawesson's reagent, PhMe, $110^\circ C$, 16 h, 96%; v) 5 equiv. Se, CD_2Cl_2 , $25^\circ C$, 16 h, 54% isolated yield; vi) 1 equiv. $MesN_3$, PhMe, $110^\circ C$, 2 h, 70%.

compounds in the case of oxygen and sulfur, while selenophosphorane formation has been reported numerous times.^[8,10] Uhl

and co-workers demonstrated that the reaction of a phosphine ligated by a CCC pincer ligand with selenium and sulfur triggered P–C bond insertion reactions.^[31] Reaction of ONO and NPN pincer compounds towards oxygen and oxygen atom transfer reagents was reported to result in ligand disassembly and ligand oxidation, respectively.^[21,51] By contrast, a CCC ligated phosphonium cation showed phosphorus centered oxidation.^[33] When 4^{iPr} is reacted with oxygen at elevated temperatures, the phosphorus oxide **7** is formed as evidenced by $^{31}P\{^1H\}$ and 1H NMR spectroscopy (Scheme 2, $^{31}P\{^1H\}$ NMR = 37.4 ppm, 55% isolated yield). **7** can also be prepared upon reaction of 4^{iPr} with pyridine N-oxide (57% isolated yield). NMR spectroscopy further reveals that **7** exhibits C_s symmetry on the NMR timescale. The molecular structure of **7** in the solid state shows that the presence of the P=O double bond (1.468(2) Å) leads to a significant geometric distortion of the acridane ligand backbone (Figure 3). Instead of being planar, the acridane ligand adopts a bent geometry to accommodate the tetrahedral phosphorus center which exhibits a τ_4 value of 0.76.^[72] The corresponding thiophosphorane **8** can be either accessed via reaction of 4^{iPr} with elemental sulfur or upon reaction of **7** with Lawesson's reagent (Scheme 2, 96% isolated yield). Finally, the selenophosphorane **9** can be cleanly obtained upon reaction of 4^{iPr} with grey selenium (Scheme 2, 54% isolated yield). Both transformations proceed with no indications of competing P–N insertion reactions. The measured coupling constant of $^1J_{P-Se} = 919$ Hz suggest a high s-character of the phosphorus lone-pair in the parent phosphine.^[73] This value however does not necessarily provide accurate information about the s-character of the phosphorus lone pair present in 4^{iPr} since the acridane ligand heavily distorts over the course of the reaction. While the C–C and C–N bond lengths of the NNN ligand for **8** and **9** are almost identical to those of **7**, the P=E double bonds and P–N single bonds show a gradual increase upon descending group 16 (Figure 3). The $^{31}P\{^1H\}$ chemical shifts show significant differences, (**7**: 37.4 ppm; **8**: 83.8 ppm, **9**: 75.7 ppm) while the 1H NMR signals are almost unchanged.

Two-electron oxidation of the phosphorus center was also observed upon reaction with $MesN_3$ (Mes = 2,4,6-Me₃-C₆H₂) to give the iminophosphorane **10** in 70% isolated yield ($^{31}P\{^1H\}$

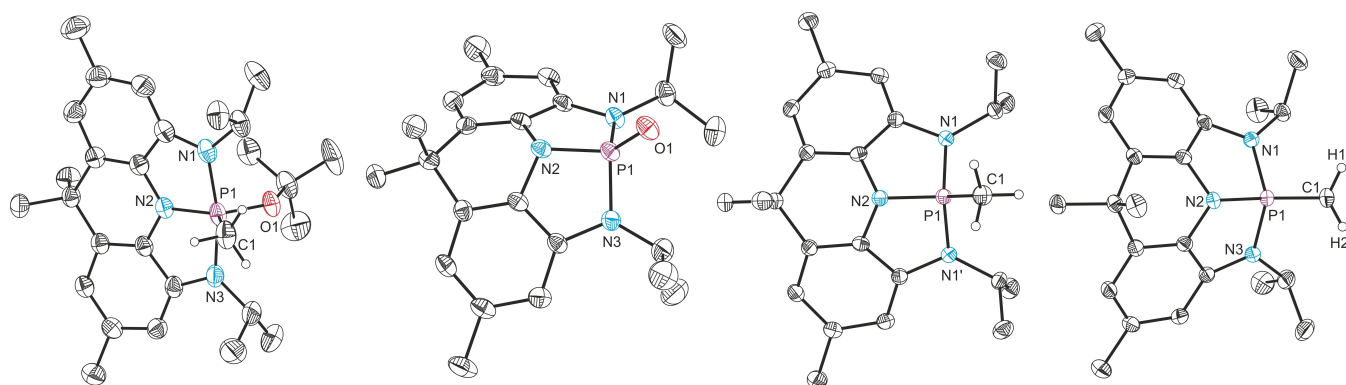


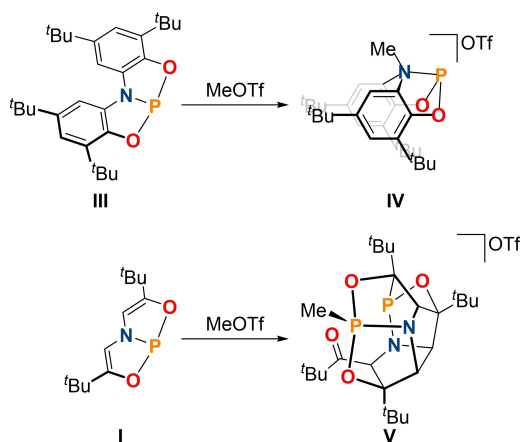
Figure 3. From left to right: single crystal X-ray structures of **6**, **7**, **11** and **12**. Thermal ellipsoids pictured at 50% probability level. Hydrogen atoms (except for those associated with C1), solvent of crystallization, and the OTf^- anion in **11** removed for clarity.

NMR 18.1 ppm, Scheme 3). As with 7–9, a geometrical distortion of the ligand backbone towards a bent shape is observed. The P=NMe_s bond length of 1.533(1) Å compares well with structurally related geometrically constrained iminophosphoranes.^[39]

Motivated by this phosphorus centered reactivity, particularly the formation of 6 through subsequent reaction with nucleophilic/electrophilic reagents, we investigated whether 6 can also be obtained via the reverse addition of these reagents. Namely, subsequent reaction of 4^{Pr} with MeOTf followed by addition of KO^tBu. It has been shown that treatment of geometrically constrained phosphines with strong electrophiles such as MeOTf resulted in ligand functionalization as was the case with bent (C_s symmetric) phosphine III and T-shaped (C_{2v} symmetric) I (Scheme 3).^[20,25,51]

In the latter case, initial phosphorus-centered reactivity was followed by disintegration of the pincer framework to provide V; a detrimental reactivity pathway that we aimed to avoid using the more chemically inert acridane backbone of 4^{Pr}. In stark contrast, 4^{Pr} reacts cleanly with MeOTf at elevated temperatures to give the phosphonium cation 11 as indicated by multinuclear NMR spectroscopy and single crystal X-ray diffraction (³¹P{¹H} NMR 80.5 ppm, Scheme 2, Figure 3, 52% isolated yield). As observed for compounds 7–9, the NNN pincer scaffolds exhibits a high degree of distortion to accommodate the cationic phosphorus center. This is accompanied by a significant shortening of the P–N bonds which lie between the values measured for of 4^{Pr} and 7. We attribute this unique electrophilic phosphorus-centered reactivity to the effective quenching of the nucleophilicity of the adjacent nitrogen due to the high rigidity of the acridane ligand framework (and thus delocalization of the nitrogen lone pairs).

Interestingly, reacting 11 with KO^tBu does not give 6 but rather yields a new product with a ³¹P{¹H} NMR chemical shift of 61.2 ppm. The presence of a new resonance in the ¹H NMR spectrum at 1.20 ppm displaying strong coupling to phosphorus (²J_{H,P} = 18.5 Hz) confirms the formation of the geometrically constrained ylid 12. This is further corroborated



Scheme 3. Previously reported ligand centered (top) and domino reactivity (bottom) of the phosphorus pincer compounds I and III upon reaction with MeOTf.

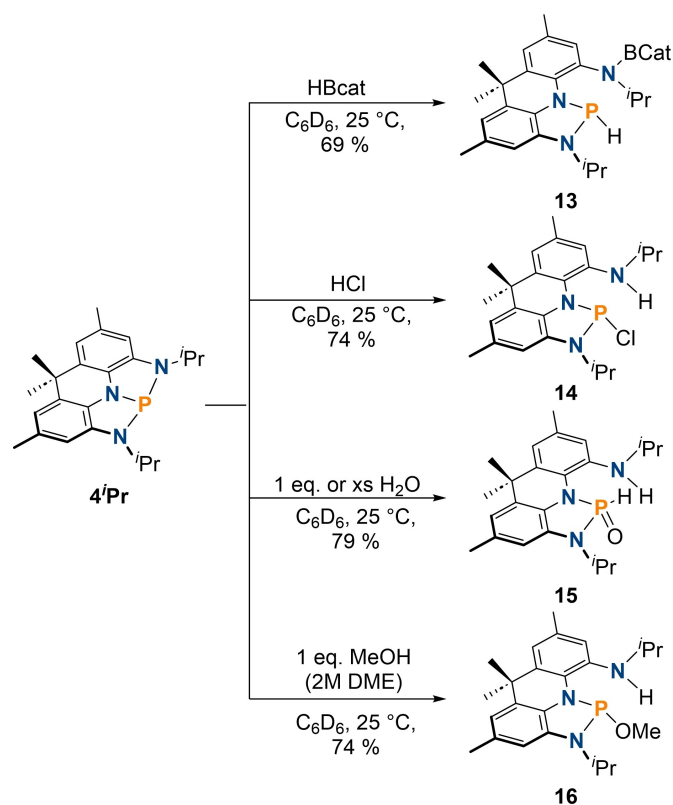
by single crystal X-ray diffraction (Scheme 2, 69% isolated yield, Figure 3). To accommodate the ylid functionality, the acridane ligand maintains its bowl shape (Figure 3). The ylidic P–CH₂ bond length (1.638(2) Å) compares well with other reported acyclic ylids,^[74,75] and is notably shorter than the P–CH₃ bond in 11 (1.778(2) Å), lying between the expected values for single and double bonds. The typical reactivity of phosphorus ylids is maintained upon geometric constraint as evidenced by reaction with benzaldehyde (Scheme 2); ³¹P{¹H} NMR spectroscopy reveals the formation of phosphine oxide 7, and the ¹H NMR spectrum displays signals corresponding to styrene (Figures S67 and S68) along with a mixture of unknown secondary products.

Reactivity towards E–H bonds

Having established the phosphorus-centered reactivity and accessibility of phosphorus(V) species derived from 4^{Pr}, we set out to evaluate its reactivity towards hydridic and protic E–H bonds. Transition metal pincer complexes are well known to undergo redox neutral, cooperative substrate activation,^[76–82] while pincer type phosphines tend to favor oxidative addition product formation due to the high stability of the phosphorus(V) redox state.^[6–10] Reacting 4^{Pr} with catecholborane (HBcat) results in the formation of two new signals in the ³¹P{¹H} NMR spectrum at 67.1 ppm and 61.8 ppm in a 1:0.6 ratio. These signals display doublet of doublet multiplicity, with a large coupling of ¹J_{H,P} = 135 and 148 Hz for the major and minor isomers respectively, and a smaller coupling of ³J_{H,P} = 11 and 12 Hz corresponding to ligand protons. This multiplicity, along with ¹H NMR spectroscopy suggests that cooperative addition along a P–N bond occurred producing two isomers of 13 containing a P–H bond (Scheme 4). This compares well with prior results obtained for bent NNN pincer compounds.^[40,41] Heating a solution of 13 in benzene at 80 °C for several days does not result in the formation of phosphorus(V) products, but rather in formation of PH₃ and 4^{Pr} suggesting that formal oxidative addition of HBcat is thermodynamically disfavored (Figure S70). Despite numerous attempts, suitable crystals for X-ray diffraction could not be obtained.

Regarding reactivity with protic E–H bonds, the reaction of 4^{Pr} with one equivalent ethereal HCl results in clean conversion to a single new product as observed by ³¹P{¹H} NMR spectroscopy (130.6 ppm, 74% isolated yield). This distinct chemical shift and the presence of a highly asymmetric ligand environment indicated by ¹H NMR spectroscopy suggests oxidative addition did not take place but rather that redox neutral substrate activation upon scission of a P–N bond occurred (Scheme 4). Single crystal X-ray diffraction corroborates these results and reveals that the reaction yielded the chlorophosphine 14 under retention of the planarity of the acridane scaffold (Figure 4). Extended heating of solutions of 14 do not result in formation of phosphorus(V) products confirming that 14 is the thermodynamically favored reaction product.

Since cooperative activation of E–H bonds along the side-arm P–N bond of 4^{Pr} appears to be the favored mode of substrate activation, we were interested if E–H bond activation



Scheme 4. Reactivity of **4^{iPr}** towards hydric and protic E–H bonds to generate **13** (only one isomer shown), **14**, **15** and **16**.

can further lead to phosphorus oxidation when multiple bonds of a substrate are cleaved. Consequently, we chose water as a simple substrate containing two acidic O–H bonds. Arduengo reported that **I** undergoes complete disassembly upon reaction with water resulting in the formation of H_3PO_3 and the fully protonated H_3ONO ligand.^[29] In contrast, Aldridge, Goicoechea and co-workers demonstrated oxidative addition of water to the bent ONO ligated phosphine **III**, yielding a hydroxo hydrido phosphorane.^[19] When **4^{iPr}** is exposed to an excess or one equivalent of water, formation of a new species in the $^{31}P\{^1H\}$ NMR spectrum at 1.3 ppm is observed suggesting the formation of a phosphorus(V) species. Furthermore, the signal is split into a doublet of doublets with observed coupling constants of $^1J_{H-P} = 715$ Hz and $^3J_{H-P} = 18$ Hz indicative of the presence of a P–H bond. 1H NMR spectroscopy ($\delta_H = 9.42$ ppm) confirms this assignment. A broad singlet resonance in the 1H NMR spectra at 3.85 ppm also indicated the formation of an N–H bond. The reaction product has an unsymmetrical 1H NMR spectra suggesting C_1 symmetry which is not in line with simple oxidative addition of water by the phosphorus center. Characteristic bands for N–H (3278 cm^{-1}) and P–H (2441 cm^{-1}) stretching vibrations are observed in the IR spectrum.

Single crystal X-ray diffraction shows that the phosphorus(V) oxide **14** was formed (Scheme 4, Figure 4, 79% isolated yield). The P=O bond length (1.4827(13) Å) is comparable with that present in **7** (cf. 1.468(2) Å). This represents a rare example of complete H_2O disassembly at a pincer-type phosphine to form

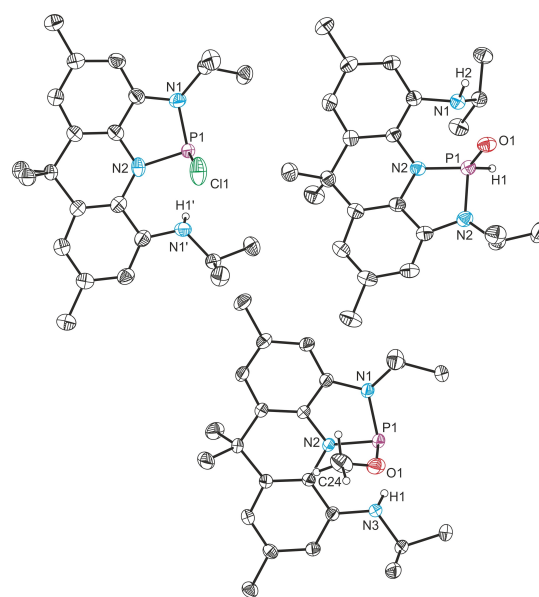


Figure 4. Clockwise from top left: single crystal X-ray structures of **14**, **15** and **16**. Thermal ellipsoids pictured at 50% probability level. Hydrogen atoms (except for those associated with activated substrates) removed for clarity.

a $P(O)HR_2$ species utilizing the ambiphilic reactivity of **4^{iPr}**.^[11,19,83–85] Reaction of **4^{iPr}** with D_2O leads to a disappearance of the P–H and N–H resonances in the 1H NMR spectra. The formation of **15** over a formal oxidative addition of water is likely to be attributed to initial cooperative splitting of an O–H bond, a reactivity typically observed for NNN phosphorus pincer compounds.^[26,28,45,47,50,55]

Consequently, we propose initial water coordination towards the highly electrophilic phosphorus center and subsequent deprotonation by the flanking nitrogen atom to afford a transient phosphinous acid. Tautomerization of R_2POH derivatives towards the corresponding oxides (to produce the final product **15** in this case) is well established if these species are not stabilized by strongly electron withdrawing ligands.^[86–92] To probe this mechanism, **4^{iPr}** is reacted with MeOH – a substrate with only one available O–H bond. Cooperative addition along a flanking P–N bond is observed to give the phosphorus(III) alkoxide **16** ($^{31}P\{^1H\}$ NMR: 97.3 ppm, Scheme 4, Figure 4, 74% isolated yield), in line with the mechanistic proposal of water activation. As in all other cases of redox neutral substrate activation, the overall planarity of the acridane ligand scaffold is maintained as evidenced by SCXRD.

Conclusion

We have reported the synthesis of the highly reactive, strictly T-shaped phosphine **4^{iPr}** ligated by a NNN pincer ligand. This was enabled by careful steric tuning of the employed acridane ligand scaffold. **4^{iPr}** exhibits pronounced ambiphilicity as evidenced by phosphorus centered reactivity towards nucleophiles and electrophiles. Furthermore, clean two electron

oxidation upon reaction with chalcogens and formation of heavily distorted tetrahedral phosphorus(V) species featuring single, double and ylidic bonds was demonstrated. Finally, the reactivity of 4^{Pr} towards hydridic and protic E–H bonds was evaluated which proceeded under retention of the phosphorus(III) redox state in case of HBCat, HCl and methanol. Finally, sequential O–H bond scission of a water molecule was observed, demonstrating both ligand-cooperative bond scission and phosphorus oxidation at a single substrate. Further studies will be directed to utilize this platform for catalytic applications.

Experimental Section

For spectra and more detailed spectral assignments, please refer to the Supporting Information document.

Synthetic methods: All reactions and product manipulations were carried out using standard Schlenk-line techniques under an inert atmosphere of argon, or in a dinitrogen filled glovebox (MBraun UNilab glovebox maintained at <0.1 ppm H₂O and <0.1 ppm O₂). Hexane (Sigma Aldrich, HPLC grade), pentane (Sigma Aldrich, HPLC grade), benzene (Rathburn, HPLC grade), dichloromethane (Sigma Aldrich, HPLC grade), acetonitrile (Sigma Aldrich, HPLC grade) diethyl ether (Sigma Aldrich, HPLC grade) and toluene (Sigma Aldrich, HPLC grade) were purified using an MBraun SPS-800 solvent system. Ethyl acetate (Sigma Aldrich, HPLC grade) and methanol (Sigma Aldrich anhydrous, 99.8%) was used as provided. THF (Sigma Aldrich, HPLC grade) was distilled over sodium/benzophenone. C₆D₆ (Sigma Aldrich, 99.5%) and CD₂Cl₂ (Sigma Aldrich, 99.5%) was degassed and dried over CaH₂. d₈-THF (Sigma Aldrich, 99.5%) was degassed and dried over sodium/potassium alloy. All dry solvents were stored under argon in gas-tight ampoules over activated 3 Å molecular sieves. 2,7,9,9-tetramethyl-4,5-dinitro-9,10-dihydroacridine,^[62] $1^{Pr[62]}$ and mesityl azide^[93] were synthesised according to their referenced literature procedures. The following were used as received from their commercial supplier without further purification: palladium on carbon (10 w%, Sigma Aldrich), H₂ (Sigma Aldrich), paraformaldehyde (Merck), sodium methoxide (Sigma Aldrich), sodium borohydride (Sigma Aldrich), phosphorus pentabromide (Acros), trimethylphosphine (Strem), magnesium powder (Sigma Aldrich), potassium *tert*-butoxide (Sigma Aldrich), 4,7,13,16,21,24-hexaoxa-1,10-diazabicyclo[8.8.8]hexacosane (Merck), methyl triflate (Apollo Scientific), oxygen (Linde), 2,4-bis(4-methoxyphenyl)-1,3,2,4-dithiadiphosphetane-2,4-disulfide (Alfa Aesar), sulfur (Sigma Aldrich), selenium (Sigma Aldrich), 2H-1,3,2-benzodioxaborole (Alfa Aesar), 2 M hydrochloric acid in diethyl ether (diluted prior to use, Alfa Aesar) and deuterium oxide (Sigma Aldrich). Phosphorus trichloride (Sigma Aldrich) was distilled and degassed prior to use. Triethylamine (TEA) was degassed, dried over CaH₂ and distilled prior to use. Benzaldehyde (Sigma Aldrich) was distilled prior to use. Pyridine N-oxide (Sigma Aldrich) was sublimed prior to use.

Characterisation techniques: NMR samples were prepared inside an inert atmosphere glovebox in NMR tubes fitted with a gas-tight valve. NMR spectra were acquired on either a Bruker AVIII 400 MHz NMR spectrometer (¹H 400 MHz, ¹¹B 128 MHz, ³¹P 162 MHz), a Bruker AVIII 500 spectrometer (¹H 500 MHz, ³¹P 202 MHz, ¹⁹F 470 MHz, ⁷⁷Se 95 MHz) or a Bruker Avance NEO 600 MHz NMR spectrometer with a broadband helium cryoprobe (¹H 600 MHz, ³¹P 243 MHz, ¹³C 151 MHz). ¹H and ¹³C NMR spectra were referenced to their respective solvent resonance (¹H NMR C₆D₆: δ = 7.16 ppm, CD₂Cl₂: δ = 5.32 ppm, d₈-THF: δ = 3.58 ppm; ¹³C NMR C₆D₆: δ = 128.1 ppm, CD₂Cl₂: δ = 53.8 ppm, d₈-THF: δ = 67.6 ppm). ¹¹B NMR spectra were

externally referenced to BF₃·Et₂O in C₆D₆. ¹⁹F NMR spectra were externally referenced to CFCI₃. ³¹P NMR spectra were externally referenced to an 85% solution of H₃PO₄ in H₂O. High-resolution mass spectrometry was acquired using a Thermo Exactive High-Resolution Orbitrap FTMS instrument equipped with a Acquity TUV Detector, with a Waters Acquity Ultraperformance LC system used for sample delivery. Elemental analyses were carried out by Elemental Analysis Services Team (London Metropolitan University, U.K.). Samples (approx. 5 mg) were submitted in flame sealed glass tubes. Infrared spectra were acquired on a Thermo Scientific iS5 FTIR spectrometer using an iD3 ATR stage.

Synthesis of 1^{Me}: 2,7,9,9-tetramethyl-4,5-dinitro-9,10-dihydroacridine (663 mg, 2.03 mmol, 1.00 equiv.) and palladium on carbon (108 mg, 0.102 mmol palladium, 10.0 wt.% palladium, 5.00 mol% palladium) are added to a gas tight ampoule and suspended in ethyl acetate (20 mL). The suspension is freeze-pump-thaw degassed four times, then refilled with dihydrogen gas (1 atm, excess) and stirred at 50 °C for 18 h. The mixture is cooled to room temperature and the solvent is removed *in vacuo*. The residue is extracted into methanol (3 × 10 mL) and filtered. The mixture is cooled to 0 °C then paraformaldehyde (608 mg, 20.6 mmol, 10.0 equiv.) is added followed by sodium methoxide (25 w% in methanol, 1.85 mL, 8.10 mmol, 4.00 equiv.). The mixture is warmed to reflux and stirred for 1 h. The mixture is then cooled to 0 °C and sodium borohydride (843 mg, 22.3 mmol, 11.0 equiv.) is added in three portions over the course of 15 min. The mixture is warmed to reflux and stirred for 2 h. The mixture is cooled to room temperature and the solvent is removed *in vacuo*. The residue is extracted into benzene (3 × 10 mL) and filtered. Lyophilisation from a concentrated benzene solution affords 1^{Me} (474 mg, 1.61 mmol, 79%) as a white powder. ¹H NMR (600 MHz, C₆D₆): δ = 6.94 (2H, s, Ar), 6.46 (2H, s, Ar), 5.69 (1H, br s, NH), 2.55 (2H, br m, NH), 2.46 (6H, d, ³J_{H-H} = 5.5 Hz, NCH₃), 2.36 (6H, s, ArCH₃), 1.73 ppm (6H, s, CH₃). ¹³C {¹H} NMR (151 MHz, C₆D₆): δ = 136.3 (s, Ar), 129.7 (s, Ar), 129.2 (s, Ar), 126.7 (s, Ar), 117.5 (s, Ar), 111.3 (s, Ar), 36.2 (s, C(CH₃)₂), 31.9 (s, CH₃), 31.1 (s, NCH₃), 21.5 ppm (s, ArCH₃). HRMS (ESI) *m/z* calcd. for C₁₉H₂₅N₃ + H⁺: 296.2121 [*M* + H]⁺; found: 296.2116.

Synthesis of 2: 1^{Me} (50.0 mg, 0.169 mmol, 1.00 equiv.) is dissolved in dichloromethane (5 mL) and cooled to –78 °C. Phosphorus trichloride (0.573 M in hexane, 0.30 mL, 0.169 mmol, 1.00 equiv.) is added followed by triethylamine (83.0 μL, 0.593 mmol, 3.50 equiv.). The mixture is gradually warmed to room temperature and stirred for 16 h, resulting in the generation of a pale-yellow solution and off-white precipitate. The solution is then filtered, and the precipitate extracted with dichloromethane (3 × 2 mL). The solvent is removed from the combined extracts *in vacuo* and the resulting residue washed with acetonitrile (3 × 2 mL) at –30 °C. The product is dried under vacuum, providing 2 as a white powder (26.0 mg, 41.1 μmol, 49%). ¹H NMR (600 MHz, C₆D₆): δ = 7.19 (1H, s, Ar), 6.85 (1H, s, Ar), 6.72 (1H, s, Ar), 6.26 (1H, s, Ar), 2.79 (6H, d, ³J_{P-H} = 8.0 Hz, NCH₃), 2.63 (6H, d, ³J_{P-H} = 1.3 Hz, NCH₃), 2.41 (6H, s, ArCH₃), 2.24 (6H, s, ArCH₃), 1.78 (6H, s, CH₃), 1.65 ppm (6H, s, CH₃). ¹H{³¹P} NMR (500 MHz, C₆D₆): as above, except δ = 2.79 (6H, s, NCH₃), 2.63 ppm (6H, s, NCH₃). ¹³C{¹H} NMR (151 MHz, C₆D₆): δ = 139.2 (d, ²J_{C-P} = 7.9 Hz, Ar), 133.8 (dd, ²J_{C-P} = 5.2 Hz, ³J_{C-P} = 2.7 Hz, Ar), 133.2 (m, C_{Ar}), 131.0 (s, Ar), 129.9 (d, ⁴J_{C-P} = 2.5 Hz, Ar), 129.2 (d, ²J_{C-P} = 8.2 Hz, Ar), 127.5 (d, ³J_{C-P} = 7.0 Hz, Ar), 126.3 (d, ⁴J_{C-P} = 2.6 Hz, Ar), 126.2 (s, C_{Ar}), 115.3 (s, Ar), 105.4 (s, Ar), 36.8 (s, C(CH₃)₂), 36.6 (s, CH₃), 34.7 (dd, ⁵J_{C-P} = 5.5 Hz, ²J_{C-P} = 13.7 Hz, NCH₃), 32.1 (d, ²J_{C-P} = 32.2 Hz, NCH₃), 31.9 (s, CH₃), 22.1 (s, ArCH₃), 21.0 ppm (s, ArCH₃). ³¹P NMR (243 MHz, C₆D₆): δ = 112.1 ppm (m). ³¹P{¹H} NMR (162 MHz, C₆D₆): δ = 112.1 ppm (s). Elemental analysis calcd. (%) for C₃₈H₄₄N₆P₂: C 70.57, H 6.86, N 12.99; found: C 70.63, H 7.01, N 11.45.

Synthesis of 3^{Me}: Phosphorus pentabromide (72.9 mg, 0.169 mmol, 1.00 equiv.) is dissolved in toluene (10 mL) and cooled to –78 °C.

Triethylamine (71.0 μL , 0.507 mmol, 3.00 equiv.) is added. A solution of 1^{Me} (50 mg, 0.169 mmol, 1.00 equiv.) in toluene (10 mL) is also cooled to -78°C and added dropwise to the phosphorus pentabromide solution. The mixture is gradually warmed to room temperature and stirred for 16 h resulting in the generation of an orange solution and off-white precipitate. The solution is then filtered, and the precipitate extracted with toluene (3 \times 5 mL). The solvent is removed *in vacuo* and the residue dissolved in hexane and cooled to -30°C for 5 days resulting in the generation of orange solid (an unknown impurity). The solution is then filtered, and the solvent removed *in vacuo*. Lyophilisation from a concentrated benzene solution provides 3^{Me} as an orange powder (52.0 mg, 0.108 mmol, 64%). ^1H NMR (600 MHz, C_6D_6): δ = 6.67 (2H, s, Ar), 6.12 (2H, s, Ar), 2.95 (6H, d, $^3J_{\text{P-H}} = 21.1$ Hz, NCH_3), 2.26 (6H, s, ArCH_3), 1.51 ppm (6H, s, CH_3). $^1\text{H}\{^{31}\text{P}\}$ NMR (500 MHz, C_6D_6): as above, expect δ = 2.95 ppm (6H, s, NCH_3). $^{13}\text{C}\{^1\text{H}\}$ NMR (151 MHz, C_6D_6): δ = 135.1 (d, $^2J_{\text{C-P}} = 12.2$ Hz, Ar), 133.6 (s, Ar), 129.7 (d, $^3J_{\text{C-P}} = 9.2$ Hz, Ar), 116.5 (d, $^4J_{\text{C-P}} = 1.8$ Hz, Ar), 116.1 (d, $^2J_{\text{C-P}} = 13.4$ Hz, Ar), 105.4 (d, $^3J_{\text{C-P}} = 7.6$ Hz, Ar), 36.9 (d, $^4J_{\text{C-P}} = 1.7$ Hz, $\text{C}(\text{CH}_3)_2$), 32.6 (s, CH_3), 31.5 (d, $^2J_{\text{C-P}} = 5.5$ Hz, NCH_3), 22.6 ppm (s, ArCH_3). ^{31}P NMR (243 MHz, C_6D_6): δ = -107.5 ppm (sept, $^3J_{\text{P-H}} = 21.1$ Hz). $^{31}\text{P}\{^1\text{H}\}$ NMR (162 MHz, C_6D_6): δ = -107.6 ppm (s). Elemental analysis calcd. (%) for $\text{C}_{19}\text{H}_{22}\text{Br}_2\text{N}_3\text{P}$: C 47.23, H 4.59, N 8.70; found: C 47.32, H 4.94, N 8.03.

Synthesis of 3^{Pr} : A solution of phosphorous pentabromide (366 mg, 0.853 mmol, 1.00 equiv.) in toluene (10 mL) is cooled to -78°C . Triethylamine (0.600 mL, 4.27 mmol, 5.00 equiv.) is added, followed by the addition of a -78°C solution of 1^{Pr} (300 mg, 0.853 mmol, 1.00 equiv.) in toluene (10 mL). The resulting bright green solution is gradually warmed to room temperature and stirred for 16 h over which the solution turned dark brown along with the precipitation of a light brown solid. The mixture is filtered, and the precipitate extracted with toluene (3 \times 5 mL). The solvent is removed *in vacuo* providing an orange-brown residue, which is then washed with diethyl ether (3 \times 5 mL) at -78°C . The resulting bright orange powder is dried *in vacuo* to provide 3^{Pr} (250 mg, 0.464 mmol, 54%). ^1H NMR (500 MHz, C_6D_6): δ = 6.64 (2H, s, Ar), 6.62 (2H, s, Ar), 4.74 (2H, d-sept, $^3J_{\text{P-H}} = 27.3$ Hz, $^3J_{\text{H-H}} = 6.9$ Hz, NCH), 2.26 (6H, s, ArCH_3), 1.53 (12H, d, $^3J_{\text{H-H}} = 6.9$ Hz, $\text{NC}(\text{CH}_3)$), 1.52 ppm (6H, s, CH_3). $^1\text{H}\{^{31}\text{P}\}$ NMR (500 MHz, C_6D_6): as above, except δ = 4.74 ppm (2H, sept, $^3J_{\text{H-H}} = 6.9$ Hz, NCH). $^{13}\text{C}\{^1\text{H}\}$ NMR (151 MHz, C_6D_6): δ = 133.0 (d, $^4J_{\text{C-P}} = 1.7$ Hz, Ar), 132.7 (d, $^2J_{\text{C-P}} = 13.7$ Hz, Ar), 130.4 (d, $^3J_{\text{C-P}} = 9.4$ Hz, Ar), 116.7 (d, $^2J_{\text{C-P}} = 14.3$ Hz, Ar), 115.8 (m, Ar), 107.9 (d, $^3J_{\text{C-P}} = 9.9$ Hz, Ar), 46.7 (d, $^2J_{\text{C-P}} = 6.0$ Hz, NCH), 36.7 (d, $^4J_{\text{C-P}} = 1.8$ Hz, $\text{C}(\text{CH}_3)_2$), 33.0 (s, CH_3), 22.7 (s, ArCH_3), 19.0 ppm (d, $^3J_{\text{C-P}} = 6.5$ Hz, $\text{NC}(\text{CH}_3)$). ^{31}P NMR (202 MHz, C_6D_6): δ = -120.1 ppm (t, $^3J_{\text{P-H}} = 27.3$ Hz). $^{31}\text{P}\{^1\text{H}\}$ NMR (162 MHz, C_6D_6): δ = -120.1 ppm (s). Elemental analysis calcd. (%) for $\text{C}_{23}\text{H}_{30}\text{Br}_2\text{N}_3\text{P}$: C 51.22, H 5.61, N 7.79; found: C 51.08, H 5.26, N 7.41.

Synthesis of 4^{Pr} : 3^{Pr} (200 mg, 0.371 mmol, 1.00 equiv.) is dissolved in toluene (10 mL). A solution of trimethyl-phosphine (0.19 mL, 1.85 mmol, 5.00 equiv.) in toluene (1 mL) is added and the mixture stirred for 15 min, resulting in the generation of a bright orange solution and off-white precipitate. The solution is filtered and the precipitate extracted with toluene (3 \times 5 mL). The solvent is removed *in vacuo*. Lyophilisation from a concentrated benzene solution provides 4^{Pr} as an orange powder (127 mg, 0.335 mmol, 90%). **Alternative procedure:** 3^{Pr} (100 mg, 0.185 mmol, 1.00 equiv.) and magnesium powder (92 mg, 3.709 mmol, 20.0 equiv.) is dissolved in tetrahydrofuran (5 mL) and stirred at room temperature for 15 min. The solvent is removed *in vacuo* and the product extracted into pentane (3 \times 2 mL) and filtered. The solvent is removed *in vacuo* from the combined extracts. Lyophilisation from a concentrated benzene solution provides 4^{Pr} as an orange powder (63.0 mg, 0.166 mmol, 90%). ^1H NMR (500 MHz, C_6D_6): δ = 6.86 (2H,

s, Ar), 6.79 (2H, s, Ar), 4.42 (2H, apparent sept, $^3J_{\text{H-H}} = 6.9$ Hz, NCH), 2.37 (6H, s, ArCH_3), 1.72 (6H, s, CH_3), 1.52 ppm (12H, d, $^3J_{\text{H-H}} = 6.9$ Hz, $\text{NC}(\text{CH}_3)$). $^1\text{H}\{^{31}\text{P}\}$ NMR (500 MHz, C_6D_6): as above. $^{13}\text{C}\{^1\text{H}\}$ NMR (151 MHz, C_6D_6): δ = 135.9 (d, $^2J_{\text{C-P}} = 12.6$ Hz, Ar), 133.5 (d, $^3J_{\text{C-P}} = 4.6$ Hz, Ar), 133.4 (s, Ar), 130.5 (d, $^2J_{\text{C-P}} = 11.2$ Hz, Ar), 115.7 (s, Ar), 109.1 (s, Ar), 45.1 (d, $^2J_{\text{C-P}} = 20.9$ Hz, NCH), 38.3 (s, $\text{C}(\text{CH}_3)_2$), 31.3 (s, CH_3), 23.6 (d, $^3J_{\text{C-P}} = 6.4$ Hz, $\text{NC}(\text{CH}_3)$), 22.6 ppm (s, ArCH_3). ^{31}P NMR (202 MHz, C_6D_6): δ = 145.0 ppm (br s). $^{31}\text{P}\{^1\text{H}\}$ NMR (162 MHz, C_6D_6): δ = as above. Elemental analysis calcd. (%) for $\text{C}_{23}\text{H}_{30}\text{N}_3\text{P}$: C 72.80, H 7.97, N 11.07; found: C 72.35, H 7.79, N 10.21.

Synthesis of 5: Potassium *tert*-butoxide (3.1 mg, 27.8 μmol , 1.00 equiv.) and 2,2,2-crypt (10.5 mg, 27.8 μmol , 1.00 equiv.) is dissolved in diethyl ether (0.5 mL). The resulting solution is added to 4^{Pr} (10.5 mg, 27.8 μmol , 1.00 equiv.) in a J. Young NMR tube producing a yellow solution. The solution is filtered, and half of the solvent is removed *in vacuo*. Crystallisation from this concentrated diethyl ether at room temperature yields **5** (11.0 mg, 12.7 μmol , 46%) as yellow crystals. ^1H NMR (500 MHz, d_8 -THF): δ = 5.82 (2H, s, Ar), 5.57 (2H, s, Ar), 3.70 (2H, apparent sept, $^3J_{\text{H-H}} = 6.6$ Hz, NCH), 3.37 (14H, s, crypt), 3.32 (14H, t, $^3J_{\text{H-H}} = 4.6$ Hz, crypt), 2.36 (14H, t, $^3J_{\text{H-H}} = 4.6$ Hz, crypt), 2.11 (6H, s, ArCH_3), 1.60 (3H, s, CH_3), 1.50 (3H, s, CH_3), 1.41 (6H, d, $^3J_{\text{H-H}} = 6.7$ Hz, $\text{NC}(\text{CH}_3)$), 1.35 (6H, d, $^3J_{\text{H-H}} = 6.7$ Hz, $\text{NC}(\text{CH}_3)$), 0.90 ppm (9H, s, O^tBu). $^1\text{H}\{^{31}\text{P}\}$ NMR (500 MHz, d_8 -THF): as above. $^{13}\text{C}\{^1\text{H}\}$ NMR (151 MHz, d_8 -THF): δ = 142.3 (d, $^2J_{\text{C-P}} = 13.2$ Hz, Ar), 128.0 (s, Ar), 127.9 (s, Ar), 125.3 (s, Ar), 107.0 (s, Ar), 100.8 (d, $^3J_{\text{C-P}} = 2.8$ Hz, Ar), 73.0 (d, $^2J_{\text{C-P}} = 21.6$ Hz, O^tBu), 71.3 (s, crypt), 68.5 (s, crypt), 54.8 (s, crypt), 46.8 (d, $^2J_{\text{C-P}} = 8.3$ Hz, NCH), 36.8 (m, $\text{C}(\text{CH}_3)_2$), 36.8 (s, CH_3), 33.7 (m, CH_3), 32.1 (d, $^2J_{\text{C-P}} = 4.1$ Hz, O^tBu), 23.1 (s, ArCH_3), 23.0 (d, $^3J_{\text{C-P}} = 3.3$ Hz, $\text{NC}(\text{CH}_3)$), 22.9 ppm (d, $^3J_{\text{C-P}} = 6.1$ Hz, $\text{NC}(\text{CH}_3)$). ^{31}P NMR (243 MHz, d_8 -THF): δ = 50.2 ppm (s). $^{31}\text{P}\{^1\text{H}\}$ NMR (162 MHz, d_8 -THF): δ = as above. Elemental analysis calcd. (%) for $\text{C}_{45}\text{H}_{75}\text{K}_1\text{N}_5\text{O}_7\text{P}$: C 62.26, H 8.71, N 8.07; found: C 61.81, H 8.77, N 7.52.

Synthesis of 6: Potassium *tert*-butoxide (3.12 mg, 27.8 μmol , 1.00 equiv.) and [2.2.2]-cryptand (10.5 mg, 27.8 μmol , 1.00 equiv.) is dissolved in diethyl ether (0.5 mL). The resulting solution is added to 4^{Pr} (10.5 mg, 27.8 μmol , 1.00 equiv.) in a J. Young NMR tube producing a yellow solution. The solvent is removed *in vacuo*. A solution of methyl triflate (3.0 μL , 27.8 μmol , 1.00 equiv.) in d_6 -benzene (0.5 mL) is added, producing a colourless solution. The solvent is removed *in vacuo* and the product extracted into pentane (3 \times 0.5 mL). The solvent is removed, then yellow crystals of **6** are grown from a concentrated hexane solution at -30°C (5.0 mg, 10.7 μmol , 38%). ^1H NMR (600 MHz, C_6D_6): δ = 6.64 (2H, s, Ar), 6.46 (2H, s, Ar), 3.75 (2H, apparent oct, $^3J_{\text{P-H}} = 6.7$ Hz, $^3J_{\text{H-H}} = 6.7$ Hz, NCH), 2.43 (6H, s, ArCH_3), 1.83 (3H, s, CH_3), 1.81 (3H, s, CH_3), 1.63 (3H, d, $^2J_{\text{P-H}} = 16.6$ Hz, PCH_3), 1.46 (6H, d, $^3J_{\text{H-H}} = 6.7$ Hz, $\text{NC}(\text{CH}_3)$), 1.35 (6H, d, $^3J_{\text{H-H}} = 6.8$ Hz, $\text{NC}(\text{CH}_3)$), 1.04 ppm (9H, s, O^tBu). $^1\text{H}\{^{31}\text{P}\}$ NMR (600 MHz, C_6D_6): as above, except δ = 3.75 (2H, sept, $^3J_{\text{H-H}} = 6.7$ Hz, NCH), 1.63 ppm (3H, s, PCH_3). $^{13}\text{C}\{^1\text{H}\}$ NMR (151 MHz, C_6D_6): δ = 135.2 (d, $^2J_{\text{C-P}} = 8.7$ Hz, Ar), 134.1 (d, $^2J_{\text{C-P}} = 19.2$ Hz, Ar), 131.6 (s, Ar), 128.6 (s, Ar), 118.9 (d, $^2J_{\text{C-P}} = 12.7$ Hz, Ar), 112.1 (s, Ar), 105.7 (d, $^3J_{\text{C-P}} = 4.4$ Hz, Ar), 80.0 (d, $^2J_{\text{C-P}} = 11.2$ Hz, O^tBu), 45.9 (d, $^2J_{\text{C-P}} = 2.6$ Hz, NCH), 36.4 (m, $\text{C}(\text{CH}_3)_2$), 35.2 (s, CH_3), 32.8 (s, CH_3), 30.5 (d, $^3J_{\text{C-P}} = 5.9$ Hz, O^tBu), 25.8 (d, $^1J_{\text{C-P}} = 179.4$ Hz, PCH_3), 23.0 (s, ArCH_3), 20.6 (d, $^3J_{\text{C-P}} = 2.2$ Hz, $\text{NC}(\text{CH}_3)$), 20.5 ppm (s, $\text{NC}(\text{CH}_3)$). ^{31}P NMR (243 MHz, C_6D_6): δ = -39.4 ppm (m). $^{31}\text{P}\{^1\text{H}\}$ NMR (162 MHz, C_6D_6): δ = -39.4 ppm (s). Elemental analysis calcd. (%) for $\text{C}_{28}\text{H}_{42}\text{N}_3\text{O}_3\text{P}$: C 71.92, H 9.05, N 8.99; found: C 72.20, H 9.46, N 8.47.

Synthesis of 7: 4^{Pr} (10.5 mg, 27.8 μmol , 1.00 equiv.) and pyridine-N-oxide (2.6 mg, 27.8 μmol , 1.00 equiv.) are dissolved in d_6 -benzene (0.5 mL) in a J. Young NMR tube and stirred at room temperature for 2 h. The solvent is removed *in vacuo* and the residue extracted into pentane (0.5 mL). Colourless crystals of **7** (6.3 mg, 15.9 μmol , 57%) are grown from a concentrated pentane solution at -30°C .

Alternative procedure: 4^{Pr} (7.0 mg, 18.5 μmol , 1.00 equiv.) is dissolved in tetrahydrofuran (0.5 mL) in a J. Young NMR tube. The solution is freeze-pump-thaw degassed four times then placed under an atmosphere of oxygen (1 atm., excess). The resulting dark red solution is heated at 60 °C for 16 h. The solution is then cooled to room temperature and the solvent removed *in vacuo*. The residues are extracted with pentane (3 \times 1 mL). Off-white microcrystalline material of **7** (4.0 mg, 10.1 μmol , 55%) is obtained from a concentrated pentane solution at -30°C . ^1H NMR (500 MHz, C_6D_6): $\delta = 6.56$ (2H, s, Ar), 6.32 (2H, s, Ar), 3.98 (2H, d-sept, $^3J_{\text{P-H}} = 15.4$ Hz, $^3J_{\text{H-H}} = 6.9$ Hz, NCH), 2.19 (6H, s, ArCH_3), 1.59 (3H, s, CH_3), 1.55 (3H, s, CH_3), 1.48 (6H, d, $^3J_{\text{H-H}} = 6.8$ Hz, $\text{NC}(\text{CH}_3)$), 1.35 ppm (6H, d, $^3J_{\text{H-H}} = 6.8$ Hz, $\text{NC}(\text{CH}_3)$). $^1\text{H}\{^{31}\text{P}\}$ NMR (500 MHz, C_6D_6): as above, except $\delta = 3.98$ ppm (2H, sept, $^3J_{\text{H-H}} = 6.9$ Hz, NCH). $^{13}\text{C}\{^1\text{H}\}$ NMR (151 MHz, C_6D_6): $\delta = 135.3$ (s, Ar), 135.2 (d, $J_{\text{C-P}} = 9.68$ Hz, Ar), 133.9 (s, Ar), 133.2 (d, $J_{\text{C-P}} = 8.8$ Hz, Ar), 115.8 (s, Ar), 109.9 (d, $^3J_{\text{C-P}} = 10.5$ Hz, Ar), 46.6 (d, $^2J_{\text{C-P}} = 3.5$ Hz, NCH), 40.2 (m, $\text{C}(\text{CH}_3)_2$), 26.4 (s, CH_3), 22.6 (s, CH_3), 22.3 (s, ArCH_3), 21.4 (d, $^3J_{\text{C-P}} = 1.1$ Hz, $\text{NC}(\text{CH}_3)$), 20.8 ppm (d, $^3J_{\text{C-P}} = 2.0$ Hz, $\text{NC}(\text{CH}_3)$). ^{31}P NMR (202 MHz, C_6D_6): $\delta = 37.4$ ppm (t, $^3J_{\text{P-H}} = 15.4$ Hz). $^{31}\text{P}\{^1\text{H}\}$ NMR (162 MHz, C_6D_6): $\delta = 37.4$ ppm (s). Elemental analysis calcd. (%) for $\text{C}_{23}\text{H}_{30}\text{N}_3\text{O}_1\text{P}$: C 69.85, H 7.65, N 10.63; found: C 69.19, H 7.61, N 10.09.

Synthesis of 8: **7** (6.0 mg, 15.2 μmol , 1.00 equiv.) and 2,4-bis(4-methoxyphenyl)-1,3,2,4-dithiadiphosphetane-2,4-disulfide (3.1 mg, 7.6 μmol , 0.50 equiv.) are dissolved in toluene (0.5 mL) in a J. Young NMR tube and heated to 110 °C for 16 h. Full conversion to **8** is observed by ^{31}P NMR spectroscopy. The solvent is removed *in vacuo* and the product extracted into hexane (0.5 mL). **8** was crystallised at -30°C following concentration of this hexane solution by slow evaporation (6.0 mg, 14.6 μmol , 96%). **Alternative procedure:** 4^{Pr} (15.0 mg, 39.5 μmol , 1.00 equiv.) and S_8 (6.4 mg, 0.198 mmol, 5.00 equiv.) are dissolved in d_2 -dichloromethane (0.5 mL) in a J. Young NMR tube and stirred for 4 h. Full conversion to thiophosphorane **8** is observed by $^{31}\text{P}\{^1\text{H}\}$ and ^1H NMR, however isolation of this product is hindered by co-crystallisation of sulfur. ^1H NMR (500 MHz, C_6D_6): $\delta = 6.55$ (2H, s, Ar), 6.34 (2H, s, Ar), 4.26 (2H, d-sept, $^3J_{\text{P-H}} = 15.0$ Hz, $^3J_{\text{H-H}} = 7.1$ Hz, NCH), 2.17 (6H, s, ArCH_3), 1.58 (3H, s, CH_3), 1.56 (3H, s, CH_3), 1.51 (6H, d, $^3J_{\text{H-H}} = 7.0$ Hz, $\text{NC}(\text{CH}_3)$), 1.29 ppm (6H, d, $^3J_{\text{H-H}} = 7.0$ Hz, $\text{NC}(\text{CH}_3)$). $^1\text{H}\{^{31}\text{P}\}$ NMR (500 MHz, C_6D_6): as above, except $\delta = 4.26$ ppm (2H, sept, $^3J_{\text{H-H}} = 7.0$ Hz, NCH). $^{13}\text{C}\{^1\text{H}\}$ NMR (151 MHz, C_6D_6): $\delta = 135.4$ (d, $^3J_{\text{C-P}} = 10.6$ Hz, Ar), 134.5 (s, Ar), 134.4 (d, $J_{\text{C-P}} = 12.6$ Hz, Ar), 133.8 (s, Ar), 116.1 (s, Ar) 109.9 (s, Ar), 48.4 (d, $^2J_{\text{C-P}} = 5.9$ Hz, NCH), 40.2 (s, $\text{C}(\text{CH}_3)_2$), 26.2 (s, CH_3), 22.7 (s, CH_3), 22.2 (s, ArCH_3), 20.8 (d, $^3J_{\text{C-P}} = 1.6$ Hz, $\text{NC}(\text{CH}_3)$), 20.1 ppm (d, $^3J_{\text{C-P}} = 3.5$ Hz, $\text{NC}(\text{CH}_3)$). ^{31}P NMR (202 MHz, C_6D_6): $\delta = 83.8$ ppm (t, $^3J_{\text{P-H}} = 15.0$ Hz). $^{31}\text{P}\{^1\text{H}\}$ NMR (162 MHz, C_6D_6): $\delta = 83.8$ ppm (s). HRMS (ESI) m/z calcd. for $\text{C}_{23}\text{H}_{30}\text{N}_3\text{PS} + \text{H}^+$: 412.1971 $[M + \text{H}]^+$; found: 412.1964.

Synthesis of 9: 4^{Pr} (10.0 mg, 26.4 μmol , 1.00 equiv.) and selenium powder (10.4 mg, 0.132 mmol, 5.00 equiv.) are suspended in d_2 -dichloromethane (0.5 mL) in a J. Young NMR tube and stirred for 2.5 h at room temperature. Full conversion to **9** was observed by ^{31}P NMR spectroscopy. The solvent is removed *in vacuo* and the residue is washed with hexane (0.5 mL). The product is extracted into tetrahydrofuran (0.3 mL), filtered, and crystallised by pentane vapour diffusion (2 mL). **9** is isolated as yellow crystals after one week (6.5 mg, 14.2 μmol , 54%). ^1H NMR (500 MHz, C_6D_6): $\delta = 6.55$ (2H, s, Ar), 6.36 (2H, s, Ar), 4.43 (2H, d-sept, $^3J_{\text{P-H}} = 14.6$ Hz, $^3J_{\text{H-H}} = 6.9$ Hz, NCH), 2.16 (6H, s, ArCH_3), 1.58 (3H, s, CH_3), 1.55 (3H, s, CH_3), 1.52 (6H, d, $^3J_{\text{H-H}} = 6.9$ Hz, $\text{NC}(\text{CH}_3)$), 1.27 ppm (6H, d, $^3J_{\text{H-H}} = 7.0$ Hz, $\text{NC}(\text{CH}_3)$). $^1\text{H}\{^{31}\text{P}\}$ NMR (500 MHz, C_6D_6): as above, except $\delta = 4.43$ ppm (2H, sept, $^2J_{\text{H-H}} = 7.0$ Hz, NCH). $^{13}\text{C}\{^1\text{H}\}$ NMR (151 MHz, C_6D_6): $\delta = 135.4$ (d, $^3J_{\text{C-P}} = 10.4$ Hz, Ar), 135.0 (d, $^2J_{\text{C-P}} = 3.0$ Hz, Ar), 134.0 (d, $^2J_{\text{C-P}} = 14.9$ Hz, Ar), 133.8 (s, Ar), 116.2 (s, Ar), 110.1 (d, $^3J_{\text{C-P}} = 8.6$ Hz, Ar), 47.1 (d, $^2J_{\text{C-P}} = 7.4$ Hz, NCH), 40.2 (s, $\text{C}(\text{CH}_3)_2$), 26.3

(s, CH_3), 22.6 (s, CH_3), 22.2 (s, ArCH_3), 20.7 (d, $^3J_{\text{C-P}} = 1.7$ Hz, $\text{NC}(\text{CH}_3)$), 20.0 ppm (d, $^3J_{\text{C-P}} = 3.9$ Hz, $\text{NC}(\text{CH}_3)$). ^{31}P NMR (243 MHz, C_6D_6): $\delta = 75.7$ ppm (dt, $^1J_{\text{P-}^{77}\text{Se}} = 919.2$ Hz, $^3J_{\text{P-H}} = 14.7$ Hz). $^{31}\text{P}\{^1\text{H}\}$ NMR (162 MHz, C_6D_6): $\delta = 75.6$ ppm (dt, $^1J_{\text{P-}^{77}\text{Se}} = 918.8$ Hz). ^{77}Se NMR (95 MHz, C_6D_6): $\delta = -35.4$ ppm (d, $^1J_{\text{P-}^{77}\text{Se}} = 916.8$ Hz). Elemental analysis calcd. (%) for $\text{C}_{23}\text{H}_{30}\text{N}_3\text{PSe}$: C 60.26, H 6.60, N 9.17; found: C 60.05, H 6.61, N 9.05.

Synthesis of 10: 4^{Pr} (10.5 mg, 27.8 μmol , 1.00 equiv.) is dissolved in a toluene (0.5 mL) solution of mesityl-azide (4.5 mg, 27.8 μmol , 1.00 equiv.) in a J. Young NMR tube. The solution was heated at 110 °C for 2 h generating a colourless solution. The solvent is removed *in vacuo* and the residues heated under dynamic vacuum for 30 min to remove any unreacted mesityl-azide. The residue is dissolved in hexane (0.5 mL) and crystals of **10** (10.0 mg, 19.5 μmol , 70%) were grown by slow evaporation of this hexane solution. ^1H NMR (500 MHz, C_6D_6): $\delta = 6.92$ (2H, s, Ar^{Mes}), 6.61 (2H, s, Ar), 6.44 (2H, s, Ar), 4.13 (2H, d-sept, $^3J_{\text{P-H}} = 11.7$ Hz, $^3J_{\text{H-H}} = 7.0$ Hz, NCH), 2.50 (6H, br s, CH_3^{Mes}), 2.26 (3H, d, $J_{\text{P-H}} = 2.8$ Hz, CH_3^{Mes}), 2.21 (6H, s, ArCH_3), 1.66 (3H, s, CH_3), 1.64 (3H, s, CH_3), 1.30 (6H, d, $^3J_{\text{H-H}} = 6.9$ Hz, $\text{NC}(\text{CH}_3)$), 1.17 ppm (6H, d, $^3J_{\text{H-H}} = 7.0$ Hz, $\text{NC}(\text{CH}_3)$). $^1\text{H}\{^{31}\text{P}\}$ NMR (500 MHz, C_6D_6): as above, except $\delta = 4.13$ (2H, sept, $^3J_{\text{H-H}} = 7.0$ Hz, NCH), 2.26 ppm (3H, s, CH_3^{Mes}). $^{13}\text{C}\{^1\text{H}\}$ NMR (151 MHz, C_6D_6): $\delta = 143.1$ (d, $J_{\text{C-P}} = 3.4$ Hz, Ar^{Mes}), 134.4 (d, $^3J_{\text{C-P}} = 10.0$ Hz, Ar), 133.8 (d, $^2J_{\text{C-P}} = 19.6$ Hz, Ar), 133.5 (d, $^2J_{\text{C-P}} = 7.3$ Hz, Ar), 133.5 (s, Ar), 131.3 (m, Ar^{Mes}), 129.5 (m, Ar^{Mes}), 129.0 (d, $J_{\text{C-P}} = 4.1$ Hz, Ar^{Mes}), 115.6 (s, Ar), 110.3 (d, $^3J_{\text{C-P}} = 10.4$ Hz, Ar), 47.0 (d, $^2J_{\text{C-P}} = 2.6$ Hz, NCH), 40.0 (s, $\text{C}(\text{CH}_3)_2$), 26.8 (s, CH_3), 22.5 (s, CH_3), 22.3 (s, ArCH_3), 20.95–20.88 (overlapping signals corresponding to one CH_3^{Mes} environment, and one set of $\text{NC}(\text{CH}_3)$ environments), 20.7 (s, CH_3^{Mes}), 20.0 ppm (d, $^3J_{\text{C-P}} = 4.4$ Hz, $\text{NC}(\text{CH}_3)$). ^{31}P NMR (243 MHz, C_6D_6): $\delta = 18.1$ ppm (m). $^{31}\text{P}\{^1\text{H}\}$ NMR (243 MHz, C_6D_6): $\delta = 18.1$ ppm (s). Elemental analysis calcd (%) for $\text{C}_{32}\text{H}_{41}\text{N}_4\text{P}$: C 74.97, H 8.06, N 10.93; found: C 74.91, H 8.30, N 10.54.

Synthesis of 11: 4^{Pr} (10.0 mg, 26.4 μmol , 1.00 equiv.) is dissolved in d_6 -benzene (0.5 mL) in a J. Young NMR tube. Methyl triflate (2.9 μL , 26.4 μmol , 1.0 equiv.) is added and the solution heated to 80 °C for 3 h. Yellow needle-like crystals form over the course of the reaction. The mixture is cooled gradually to room temperature and left for 16 h. The crystals are filtered, washed with benzene (3 \times 0.5 mL) and dried *in vacuo* to yield **11** (7.5 mg, 13.8 μmol , 52%). ^1H NMR (500 MHz, CD_2Cl_2): $\delta = 6.88$ (2H, s, Ar), 6.81 (2H, s, Ar), 4.55 (2H, d-sept, $^3J_{\text{P-H}} = 11.6$ Hz, $^3J_{\text{H-H}} = 6.9$ Hz, NCH), 3.13 (3H, d, $^2J_{\text{P-H}} = 15.6$ Hz, PCH_3), 2.38 (6H, s, ArCH_3), 1.82 (3H, s, CH_3), 1.70 (6H, d, $^3J_{\text{H-H}} = 7.0$ Hz, $\text{NC}(\text{CH}_3)$), 1.64 (3H, s, CH_3), 1.58 ppm (6H, d, $^3J_{\text{H-H}} = 6.8$ Hz, $\text{NC}(\text{CH}_3)$). $^1\text{H}\{^{31}\text{P}\}$ NMR (500 MHz, CD_2Cl_2): as above, except $\delta = 4.55$ (2H, sept, $^3J_{\text{H-H}} = 6.8$ Hz, NCH), 3.13 ppm (3H, s, PCH_3). $^{13}\text{C}\{^1\text{H}\}$ NMR (151 MHz, CD_2Cl_2): $\delta = 137.0$ (s, Ar), 136.4 (d, $^3J_{\text{C-P}} = 10.4$ Hz, Ar), 133.0 (d, $^4J_{\text{C-P}} = 3.0$ Hz, Ar), 131.4 (d, $^2J_{\text{C-P}} = 15.7$ Hz, Ar), 119.4 (d, $^4J_{\text{C-P}} = 1.8$ Hz, Ar), 113.0 (d, $^3J_{\text{C-P}} = 9.1$ Hz, Ar), 47.9 (d, $^2J_{\text{C-P}} = 4.1$ Hz, NCH), 40.5 (s, $\text{C}(\text{CH}_3)_2$), 26.9 (s, CH_3), 22.5 (s, CH_3), 22.2 (s, ArCH_3), 21.6 (s, $\text{NC}(\text{CH}_3)$), 21.1 (d, $^3J_{\text{C-P}} = 5.8$ Hz, $\text{NC}(\text{CH}_3)$), 16.0 ppm (d, $^1J_{\text{C-P}} = 125.1$ Hz, PCH_3). ^{31}P NMR (243 MHz, CD_2Cl_2): $\delta = 80.5$ ppm (qt, $^2J_{\text{P-H}} = 15.4$ Hz, $^3J_{\text{P-H}} = 11.6$ Hz). $^{31}\text{P}\{^1\text{H}\}$ NMR (243 MHz, CD_2Cl_2): $\delta = 80.5$ ppm (s). $^{19}\text{F}\{^1\text{H}\}$ NMR (470 MHz, CD_2Cl_2): $\delta = 78.9$ ppm (s, OTf). Elemental analysis calcd. (%) for $\text{C}_{25}\text{H}_{33}\text{F}_3\text{N}_3\text{O}_3\text{PS}$: C 55.24, H 6.12, N 7.73; found: C 55.81, H 6.07, N 7.59.

Synthesis of 12: 4^{Pr} (10.5 mg, 27.8 μmol , 1.00 equiv.) is dissolved in d_6 -benzene (0.5 mL) in a J. Young NMR tube. Methyl triflate (3.0 μL , 27.8 μmol , 1.00 equiv.) is added and the solution heated to 80 °C for 3 h. The solvent is removed *in vacuo* and the residues dissolved in a solution of potassium *tert*-butoxide (3.1 mg, 27.8 μmol , 1.00 equiv.) in tetrahydrofuran (0.5 mL). A colourless solution results. The solvent is removed *in vacuo* and the product extracted into hexane (2 \times 0.5 mL). Colourless crystals of **12** (7.6 mg, 19.3 μmol , 69%) were grown from a concentrated hexane solution at -30°C . ^1H NMR

(600 MHz, C₆D₆): δ = 6.63 (2H, s, Ar), 6.47 (2H, s, Ar), 4.23 (2H, d-sept, ³J_{P-H} = 11.4 Hz, ³J_{H-H} = 7.0 Hz, NCH), 2.26 (6H, s, ArCH₃), 1.65 (3H, s, CH₃), 1.59 (3H, s, CH₃), 1.40 (6H, d, ³J_{H-H} = 7.0 Hz, NC(CH₃)), 1.20 (2H, d, ²J_{P-H} = 18.5 Hz, PCH₂), 1.19 ppm (6H, d, ³J_{H-H} = 7.1 Hz, NC(CH₃)). ¹H {³¹P} NMR (600 MHz, C₆D₆): as above, except δ = 4.23 (2H, sept, ³J_{H-H} = 7.0 Hz, NCH), 1.20 ppm (2H, s, PCH₂). ¹³C{¹H} NMR (151 MHz, C₆D₆): δ = 133.8 (d, ²J_{C-P} = 4.1 Hz, Ar), 133.1 (d, ²J_{C-P} = 16.4 Hz, Ar), 132.9 (d, ³J_{C-P} = 10.3 Hz, Ar), 132.4 (s, Ar), 115.6 (s, Ar), 109.8 (d, ³J_{C-P} = 8.9 Hz, Ar), 47.1 (d, ²J_{C-P} = 3.9 Hz, NCH), 39.4 (s, C(CH₃)₂), 27.4 (s, CH₃), 22.8 (s, CH₃), 22.4 (s, CH₃), 20.9 (s, NC(CH₃)), 20.5 (d, ³J_{C-P} = 5.2 Hz, NC(CH₃)), 16.9 ppm (d, ¹J_{C-P} = 240.1 Hz, PCH₂). ³¹P NMR (243 MHz, C₆D₆): δ = 61.2 ppm (m). ³¹P{¹H} NMR (162 MHz, C₆D₆): δ = 61.2 ppm (s). Elemental analysis calcd. (%) for C₂₄H₃₂N₃P: C 73.25, H 8.20, N 10.68; found: C 73.63, H 8.40, N 10.16.

Synthesis of 13: 4^{Pr} (10.0 mg, 26.4 μ mol, 1.00 equiv.) is dissolved in d₆-benzene (0.5 mL) in a J. Young NMR tube. Catachole borane (2.8 μ L, 26.4 μ mol, 1.00 equiv.) is added, resulting in the immediate generation of a colourless solution. Full conversion to an isomeric mixture of **13** (1:0.6 ratio) was observed by ³¹P NMR spectroscopy. The solvent is removed *in vacuo*, dissolved in benzene and lyophilised to yield the isomeric mixture of **13** as an off white powder (9.6 mg, 19.2 μ mol, 69%). ¹H NMR (600 MHz, C₆D₆): **major isomer** δ = 7.20 (1H, s, Ar), 7.02 (1H, d, ¹J_{P-H} = 135.0 Hz, P-H), 6.91 (Ar^{BCat}), 6.86 (1H, m, Ar), 6.70 (1H, s, Ar), 6.68 (Ar^{BCat}), 6.27 (1H, s, Ar), 4.35 (1H, sept, ²J_{H-H} = 6.7 Hz, NCH), 3.54 (1H, d-sept, ³J_{P-H} = 11.6 Hz, ³J_{H-H} = 6.6 Hz, NCH), 2.30 (3H, s, ArCH₃), 2.18 (3H, s, ArCH₃), 1.71 (3H, s, CH₃), 1.51 (3H, s, CH₃), 1.43 (3H, d, ²J_{H-H} = 6.6 Hz, NC(CH₃)), 1.18 (3H, d, ²J_{H-H} = 6.8 Hz, NC(CH₃)), 1.18 (3H, d, ²J_{H-H} = 6.6 Hz, NC(CH₃)), 0.94 ppm (3H, d, ²J_{H-H} = 6.5 Hz, NC(CH₃)). **minor isomer** δ = 7.16 (Ar), 7.15 (1H, d, ¹J_{P-H} = 148.0 Hz, P-H), 6.98 (2H, br m, Ar^{BCat}), 6.91 (Ar), 6.74 (2H, dd, ³J_{H-H} = 5.7 Hz, ⁴J_{H-H} = 3.3 Hz, Ar^{BCat}), 6.66 (1H, s, Ar), 6.25 (s, 1H, Ar), 4.11 (1H, sept, ²J_{H-H} = 6.7 Hz, NCH), 3.44 (1H, d-sept, ³J_{P-H} = 12.7 Hz, ²J_{H-H} = 6.3 Hz, NCH), 2.29 (3H, s, ArCH₃), 2.18 (3H, s, ArCH₃), 1.64 (3H, s, CH₃), 1.59 (3H, s, CH₃), 1.38 (3H, d, ²J_{H-H} = 6.5 Hz, NC(CH₃)), 1.00 (3H, d, ²J_{H-H} = 6.6 Hz, NC(CH₃)), 0.90 (3H, d, ²J_{H-H} = 6.5 Hz, NC(CH₃)), 0.86 ppm (3H, d, ²J_{H-H} = 6.6 Hz, NC(CH₃)). ¹H{³¹P} NMR (500 MHz, C₆D₆): **major isomer** as above, except δ = 7.02 (1H, s, P-H), 3.54 ppm (1H, sept, ²J_{H-H} = 6.6 Hz, NCH). **minor isomer** as above, except δ = 7.15 (1H, s, P-H), 3.44 ppm (1H, sept, ²J_{H-H} = 6.3 Hz, NCH). ¹³C{¹H} NMR (151 MHz, C₆D₆): **major isomer** δ = 149.4 (s, Ar^{BCat}), 139.6 (d, ²J_{C-P} = 6.7 Hz, Ar), 135.5 (d, ²J_{C-P} = 3.6 Hz, Ar), 134.5 (d, ³J_{C-P} = 2.1 Hz, Ar), 133.3 (d, ²J_{C-P} = 9.5 Hz, Ar), 131.3 (s, Ar), 130.9 (s, Ar), 130.0 (s, Ar), 128.4 (s, Ar), 127.0 (s, Ar), 122.3 (s, Ar^{BCat}), 116.4 (s, Ar), 112.1 (s, Ar^{BCat}), 108.5 (s, Ar), 51.9 (d, ⁵T_J_{C-P} = 13.4 Hz, NCH), 47.5 (d, ²J_{C-P} = 17.4 Hz, NCH), 36.6 (s, C(CH₃)₂), 34.8 (s, CH₃), 31.5 (s, CH₃), 24.3 (s, NC(CH₃)), 22.2 (d, ³J_{C-P} = 10.9 Hz, NC(CH₃)), 21.9 (s, ArCH₃), 21.4 (s, NC(CH₃)), 20.9 (s, ArCH₃), 19.0 ppm (d, ⁶T_J_{C-P} = 6.1 Hz, NC(CH₃)). **minor isomer** δ = 149.7 (s, Ar^{BCat}), 139.5 (d, ²J_{C-P} = 6.5 Hz, Ar), 134.4 (s, Ar), 133.8 (d, ²J_{C-P} = 2.0 Hz, Ar), 132.8 (d, ²J_{C-P} = 7.8 Hz, Ar), 131.2 (s, Ar), 129.3 (s, Ar), 128.3 (s, Ar), 126.8 (s, Ar), 126.7 (s, Ar), 122.0 (s, Ar^{BCat}), 116.8 (s, Ar), 112.0 (s, Ar^{BCat}), 108.8 (s, Ar), 50.5 (s, NCH), 47.9 (d, ²J_{C-P} = 18.1 Hz, NCH), 36.7 (s, C(CH₃)₂), 34.6 (s, CH₃), 33.0 (s, CH₃), 25.1 (s, NC(CH₃)), 21.9 (s, ArCH₃), 21.6 (d, ²J_{C-P} = 12.2 Hz, NC(CH₃)), 21.3 (s, NC(CH₃)), 20.9 (s, ArCH₃), 20.6 ppm (s, NC(CH₃)). ³¹P NMR (243 MHz, C₆D₆): **major isomer** δ = 67.1 ppm (dd, ¹J_{P-H} = 135.0 Hz, ³J_{P-H} = 11.3 Hz). **minor isomer** δ = 61.8 ppm (dd, ¹J_{P-H} = 148.4 Hz, ³J_{P-H} = 12.3 Hz). ³¹P{¹H} NMR (202 MHz, C₆D₆): **major isomer** δ = 67.1 ppm (s). **minor isomer** δ = 61.8 ppm (s). ¹¹B{¹H} NMR (128 MHz, C₆D₆): δ = -28.6 (br), -34.0 ppm (br) (assignment of major and minor isomer could not be achieved).

Synthesis of 14: 4^{Pr} (10.5 mg, 27.8 μ mol, 1.00 equiv.) is dissolved in d₆-benzene (0.5 mL) in a J. Young NMR tube. Hydrochloric acid (0.2 M in diethyl ether, 0.14 mL, 27.8 μ mol, 1.00 equiv.) is added, instantly generating a colourless solution. The solvent was removed *in vacuo* and the product dissolved in pentane (0.5 mL). Pale yellow

crystals of **14** (8.5 mg, 20.4 μ mol, 74%) were grown from a concentrated pentane solution at -30 °C. ¹H NMR (500 MHz, C₆D₆): δ = 7.06 (1H, s, Ar), 6.83 (1H, s, Ar), 6.58 (1H, s, Ar), 6.55 (1H, s, Ar), 3.99 (1H, d-sept, ³J_{P-H} = 11.5 Hz, ³J_{H-H} = 6.7 Hz, NCH), 3.19 (1H, sept, ³J_{H-H} = 6.2 Hz, NCH), 2.97 (1H, br s, N-H), 2.33 (3H, s, ArCH₃), 2.19 (3H, s, ArCH₃), 1.57 (6H, br s, CH₃), 1.54 (6H, d, ³J_{H-H} = 6.6 Hz, NC(CH₃)), 1.10 ppm (6H, d, ³J_{H-H} = 6.2 Hz, NC(CH₃)). ¹H{³¹P} NMR (500 MHz, C₆D₆): as above, except δ = 3.99 ppm (1H, sept, ³J_{H-H} = 6.7 Hz, NCH). ¹³C{¹H} NMR (151 MHz, C₆D₆): δ = 134.9 (d, ²J_{C-P} = 9.8 Hz, Ar), 134.7 (d, ²J_{C-P} = 3.4 Hz, Ar), 133.6 (s, Ar), 132.4 (s, Ar), 132.3 (s, Ar), 131.2 (d, ²J_{C-P} = 8.0 Hz, Ar), 130.1 (s, Ar), 129.1 (d, ²J_{C-P} = 12.1 Hz, Ar), 125.2 (s, Ar), 125.0 (s, Ar), 117.9 (s, Ar), 109.1 (s, Ar), 49.0 (d, ⁵T_J_{C-P} = 6.0 Hz, NCH), 47.5 (d, ²J_{C-P} = 15.8 Hz, NCH), 36.4 (s, C(CH₃)₂), 22.0 (s, ArCH₃), 21.1 ppm (s, ArCH₃). ³¹P NMR (243 MHz, C₆D₆): δ = 130.6 ppm (m). ³¹P{¹H} NMR (243 MHz, C₆D₆): δ = 130.6 ppm (s). Elemental analysis calcd. (%) for C₂₃H₃₁ClN₃P: C 66.42, H 7.51, N 10.10; found: C 67.21, H 8.24, N 9.01. This is consistent with the presence of 0.5 equiv. pentane in the crystalline sample submitted.

Synthesis of 15: 4^{Pr} (31.0 mg, 81.7 μ mol, 1.00 equiv.) is dissolved in d₆-benzene (0.5 mL) in a J. Young NMR tube. Water (1.5 μ L, 81.7 μ mol, 1.00 equiv.) is added resulting in an immediate colour change to colourless. The solvent is removed *in vacuo* and the remaining residue heated under vacuum to remove traces of water. Lyophilisation from a concentrated benzene solution yields **15** as a colourless powder (25.5 mg, 64.2 μ mol, 79%). ¹H NMR (400 MHz, C₆D₆): δ = 9.42 (1H, d, ¹J_{P-H} = 714.6 Hz, P-H), 6.97 (1H, s, Ar), 6.69 (1H, s, Ar), 6.64 (1H, s, Ar), 6.29 (1H, s, Ar), 3.85 (1H, s, N-H), 3.72 (1H, d-sept, ³J_{P-H} = 18.0 Hz, ³J_{H-H} = 6.7 Hz, NCH), 3.31 (1H, sept, ³J_{H-H} = 6.3 Hz, NCH), 2.31 (3H, s, ArCH₃), 2.18 (3H, s, ArCH₃), 1.64 (3H, s, CH₃), 1.54 (3H, s, CH₃), 1.41 (3H, d, ³J_{H-H} = 6.7 Hz, NC(CH₃)), 1.40 (3H, d, ³J_{H-H} = 6.7 Hz, NC(CH₃)), 1.21 (3H, d, ³J_{H-H} = 6.3 Hz, NC(CH₃)), 0.95 ppm (3H, d, ³J_{H-H} = 6.3 Hz, NC(CH₃)). ¹H{³¹P} NMR (400 MHz, C₆D₆): as above, except δ = 9.42 (1H, s, P-H), 3.72 ppm (1H, sept, ³J_{H-H} = 6.7 Hz, NCH). ¹³C{¹H} NMR (151 MHz, C₆D₆): δ = 133.6 (s, Ar), 133.0 (d, ²J_{C-P} = 8.6 Hz, Ar), 132.9 (d, ²J_{C-P} = 5.7 Hz, Ar), 131.9 (s, Ar), 131.5 (s, Ar), 129.9 (s, Ar), 127.3 (d, ³J_{C-P} = 5.9 Hz, Ar), 125.1 (d, ²J_{C-P} = 10.8 Hz, Ar), 123.9 (s, Ar), 121.8 (s, Ar), 116.3 (s, Ar), 106.6 (d, ³J_{C-P} = 6.16 Hz, Ar), 47.0 (s, NCH), 46.3 (d, ²J_{C-P} = 5.0 Hz, NCH), 36.2 (s, C(CH₃)₂), 34.5 (s, CH₃), 34.0 (s, CH₃), 22.6 (s, NC(CH₃)), 22.1 (s, ArCH₃), 21.8 (s, NC(CH₃)), 21.2 (s, ArCH₃), 21.0 (s, NC(CH₃)), 20.0 ppm (d, ³J_{C-P} = 3.73 Hz, NC(CH₃)). ³¹P NMR (162 MHz, C₆D₆): δ = 1.3 ppm (dd, ¹J_{P-H} = 714.6 Hz, ³J_{P-H} = 18.3 Hz). ³¹P{¹H} NMR (162 MHz, C₆D₆): δ = 1.3 ppm (s). Elemental analysis calcd. (%) for C₂₃H₃₂N₃OP: C 69.50, H 8.11, N 10.57; found: C 68.72, H 7.68, N 9.97. This is consistent with the presence of 0.25 equiv. water in the crystalline sample submitted.

Synthesis of 16: 4^{Pr} (10.5 mg, 27.8 μ mol, 1.00 equiv.) is dissolved in d₆-benzene (0.5 mL) in a J. Young NMR tube. Methanol (2 M in DME, 14.0 μ L, 27.8 μ mol, 1.00 equiv.) is added resulting in the generation of a pale-yellow solution. The solvent is removed *in vacuo* and the residue extracted with pentane (2 \times 0.5 mL). Crystals of **16** (8.5 mg, 20.7 μ mol, 74%) are grown from a concentrated pentane solution at -30 °C. ¹H NMR (600 MHz, C₆D₆): δ = 7.02 (1H, s, Ar), 6.79 (1H, s, Ar), 6.57 (1H, s, Ar), 6.43 (1H, s, Ar), 3.92 (1H, d-sept, ³J_{P-H} = 10.2 Hz, ³J_{H-H} = 6.7 Hz, NCH), 3.47 - 3.39 (2H, N-H and NCH), 2.81 (3H, d, ³J_{P-H} = 7.4 Hz, OCH₃), 2.39 (3H, s, ArCH₃), 2.28 (3H, s, ArCH₃), 1.76 (3H, s, CH₃), 1.72 (3H, s, CH₃), 1.43 (3H, dd, ³J_{H-H} = 6.7 Hz, ⁴J_{P-H} = 1.1 Hz, NC(CH₃)), 1.38 (3H, d, ³J_{H-H} = 6.7 Hz, NC(CH₃)), 1.19 - 1.17 ppm (6H, NCH(CH₃)). ¹H{³¹P} NMR (600 MHz, C₆D₆): as above, except δ = 3.92 (1H, sept, ³J_{H-H} = 6.7 Hz, NCH), 2.81 (3H, s, OCH₃), 1.43 ppm (3H, d, ³J_{H-H} = 6.7 Hz, NC(CH₃)). ¹³C{¹H} NMR (151 MHz, C₆D₆): δ = 136.4 (d, ²J_{C-P} = 7.8 Hz, Ar), 134.4 (d, ³J_{C-P} = 1.5 Hz, Ar), 133.4 (d, ³J_{C-P} = 2.1 Hz, Ar), 130.8 (s, Ar), 130.7 (s, Ar), 130.1 (d, ²J_{C-P} = 8.8 Hz, Ar), 128.6 (s, Ar), 127.0 (s, Ar), 121.3 (s, Ar), 119.0 (s, Ar), 116.2 (s, Ar), 106.1 (s, Ar), 49.7 (d, ²J_{C-P} = 5.4 Hz, OCH₃), 46.7 (d, ²J_{C-P} =

19.5 Hz, NCH), 46.5 (d, ^{57}S , $J_{\text{C-P}} = 5.9$ Hz, NCH), 36.6 (s, $\text{C}(\text{CH}_3)_2$), 34.7 (s, CH_3), 34.6 (s, CH_3), 22.7 - 22.6 (overlapping multiplets, $\text{NC}(\text{CH}_3)$), 22.4 (s, $\text{NC}(\text{CH}_3)$), 22.1 (s, ArCH_3), 21.3 ppm (s, ArCH_3). ^{31}P NMR (243 MHz, C_6D_6): $\delta = 97.3$ ppm (m). $^{31}\text{P}\{^1\text{H}\}$ NMR (243 MHz, C_6D_6): $\delta = 97.3$ ppm (s). Elemental analysis calcd. (%) for $\text{C}_{24}\text{H}_{34}\text{N}_3\text{O}$: C 70.05, H 8.33, N 10.21; found: C 70.15, H 8.44, N 9.80.

Acknowledgements

We thank the Deutsche Forschungsgemeinschaft (DFG; AB 820/1-1 and Rückkehrstipendium; J.A.) and the EPSRC Oxford Inorganic Chemistry for Future Manufacturing CDT (OxICFM; EP/S023828/1; A.J.K.) for funding this research. The University of Oxford are also acknowledged for access to Chemical Crystallography and NMR facilities.

Conflict of Interests

The authors declare no conflict of interest.

Data Availability Statement

The data that support the findings of this study are available in the supplementary material of this article.

Keywords: cooperativity · phosphorus · pincer ligands · small molecule activation · water activation

- [1] P. P. Power, *Nature* **2010**, *463*, 171–177.
- [2] T. Chu, G. I. Nikonov, *Chem. Rev.* **2018**, *118*, 3608–3680.
- [3] C. Weetman, S. Inoue, *ChemCatChem* **2018**, *10*, 4213–4228.
- [4] R. L. Melen, *Science* **2019**, *363*, 479–484.
- [5] C. Weetman, *Chem. Eur. J.* **2021**, *27*, 1941–1954.
- [6] J. M. Lipschultz, G. Li, A. T. Radosevich, *J. Am. Chem. Soc.* **2021**, *143*, 1699–1721.
- [7] J. Abbenseth, J. M. Goicoechea, *Chem. Sci.* **2020**, *11*, 9728–9740.
- [8] S. Kundu, *Chem. Asian J.* **2020**, *15*, 3209–3224.
- [9] A. Brand, W. Uhl, *Chem. Eur. J.* **2019**, *25*, 1391–1404.
- [10] L. Greb, F. Ebner, Y. Ginzburg, L. M. Sigmund, *Eur. J. Inorg. Chem.* **2020**, 3030–3047.
- [11] L. Wang, Y. Li, Z. Li, M. Kira, *Coord. Chem. Rev.* **2022**, *457*, 214413.
- [12] Y. Mizuhata, T. Sasamori, N. Tokitoh, *Chem. Rev.* **2009**, *109*, 3479–3511.
- [13] D. Bourissou, O. Guerret, F. P. Gabbaï, G. Bertrand, *Chem. Rev.* **2000**, *100*, 39–92.
- [14] M. S. Nechaev, *Organometallics* **2021**, *40*, 3408–3423.
- [15] C. Bonningue, D. Houalla, M. Sanchez, R. Wolf, F. H. Osman, *J. Chem. Soc. Perkin Trans. 2* **1981**, 19–25.
- [16] C. Bonningue, D. Houalla, R. Wolf, J. Jaud, *J. Chem. Soc. Perkin Trans. 2* **1983**, 773–776.
- [17] D. Houalla, F. H. Osman, M. Sanchez, R. Wolf, *Tetrahedron Lett.* **1977**, *18*, 3041–3044.
- [18] S. A. Culley, A. J. Arduengo, *J. Am. Chem. Soc.* **1984**, *106*, 1164–1165.
- [19] T. P. Robinson, D. M. De Rosa, S. Aldridge, J. M. Goicoechea, *Angew. Chem. Int. Ed.* **2015**, *54*, 13758–13763.
- [20] T. P. Robinson, S.-K. Lo, D. De Rosa, S. Aldridge, J. M. Goicoechea, *Chem. Eur. J.* **2016**, *22*, 15712–15724.
- [21] T. P. Robinson, D. De Rosa, S. Aldridge, J. M. Goicoechea, *Chem. Eur. J.* **2017**, *23*, 15455–15465.
- [22] P. Wang, Q. Zhu, Y. Wang, G. Zeng, J. Zhu, C. Zhu, *Chin. Chem. Lett.* **2021**, *32*, 1432–1436.
- [23] A. J. Pistner, H. W. Moon, A. Silakov, H. P. Yennawar, A. T. Radosevich, *Inorg. Chem.* **2017**, *56*, 8661–8668.
- [24] S. M. McCarthy, Y.-C. Lin, D. Devarajan, J. W. Chang, H. P. Yennawar, R. M. Rioux, D. H. Ess, A. T. Radosevich, *J. Am. Chem. Soc.* **2014**, *136*, 4640–4650.
- [25] M. Driess, N. Muresan, K. Merz, M. Päch, *Angew. Chem. Int. Ed.* **2005**, *44*, 6734–6737.
- [26] G. Zeng, S. Maeda, T. Taketsugu, S. Sakaki, *Angew. Chem. Int. Ed.* **2014**, *53*, 4633–4637.
- [27] S. Volodarsky, R. Dobrovetsky, *Chem. Commun.* **2018**, *54*, 6931–6934.
- [28] A. Pal, K. Vanka, *Inorg. Chem.* **2016**, *55*, 558–565.
- [29] A. J. Arduengo, C. A. Stewart, *Chem. Rev.* **1994**, *94*, 1215–1237.
- [30] D. Bawari, S. Volodarsky, Y. Ginzburg, K. Jaiswal, P. Joshi, R. Dobrovetsky, *Chem. Commun.* **2022**, *58*, 12176–12179.
- [31] A. Hentschel, A. Brand, P. Wegener, W. Uhl, *Angew. Chem. Int. Ed.* **2018**, *57*, 832–835.
- [32] A. Brand, P. Wegener, A. Hepp, W. Uhl, *Organometallics* **2020**, *39*, 1384–1392.
- [33] K. Chulsky, I. Malahov, D. Bawari, R. Dobrovetsky, *J. Am. Chem. Soc.* **2023**, *145*, 3786–3794.
- [34] M. B. Kindervater, K. M. Marczenko, U. Werner-Zwanziger, S. S. Chitnis, *Angew. Chem. Int. Ed.* **2019**, *58*, 7850–7855.
- [35] G. T. Cleveland, A. T. Radosevich, *Angew. Chem. Int. Ed.* **2019**, *58*, 15005–15009.
- [36] N. L. Dunn, M. Ha, A. T. Radosevich, *J. Am. Chem. Soc.* **2012**, *134*, 11330–11333.
- [37] K. Lee, A. V. Blake, A. Tanushi, S. M. McCarthy, D. Kim, S. M. Loria, C. M. Donahue, K. D. Spielvogel, J. M. Keith, S. R. Daly, A. T. Radosevich, *Angew. Chem. Int. Ed.* **2019**, *58*, 6993–6998.
- [38] S. Lim, A. T. Radosevich, *J. Am. Chem. Soc.* **2020**, *142*, 16188–16193.
- [39] Y.-C. Lin, J. C. Gilhula, A. T. Radosevich, *Chem. Sci.* **2018**, *9*, 4338–4347.
- [40] Y.-C. Lin, E. Hatzakis, S. M. McCarthy, K. D. Reichl, T.-Y. Lai, H. P. Yennawar, A. T. Radosevich, *J. Am. Chem. Soc.* **2017**, *139*, 6008–6016.
- [41] J. M. Lipschultz, Y. Fu, P. Liu, A. T. Radosevich, *Chem. Sci.* **2021**, *12*, 1031–1037.
- [42] H. W. Moon, A. Maity, A. T. Radosevich, *Organometallics* **2021**, *40*, 2785–2791.
- [43] A. Tanushi, A. T. Radosevich, *J. Am. Chem. Soc.* **2018**, *140*, 8114–8118.
- [44] C. te Grotenhuis, J. T. Mattos, A. T. Radosevich, *Phosphorus Sulfur Silicon Relat. Elem.* **2020**, *195*, 940–946.
- [45] W. Zhao, S. M. McCarthy, T. Y. Lai, H. P. Yennawar, A. T. Radosevich, *J. Am. Chem. Soc.* **2014**, *136*, 17634–17644.
- [46] M. K. Mondal, L. Zhang, Z. Feng, S. Tang, R. Feng, Y. Zhao, G. Tan, H. Ruan, X. Wang, *Angew. Chem. Int. Ed.* **2019**, *58*, 15829–15833.
- [47] S. Volodarsky, D. Bawari, R. Dobrovetsky, *Angew. Chem. Int. Ed.* **2022**, *61*, e202208401.
- [48] Q. J. Bruch, A. Tanushi, P. Müller, A. T. Radosevich, *J. Am. Chem. Soc.* **2022**, *144*, 21443–21447.
- [49] S. J. Hwang, A. Tanushi, A. T. Radosevich, *J. Am. Chem. Soc.* **2020**, *142*, 21285–21291.
- [50] J. Cui, Y. Li, R. Ganguly, A. Inthirarajah, H. Hirao, R. Kinjo, *J. Am. Chem. Soc.* **2014**, *136*, 16764–16767.
- [51] J. Cui, Y. Li, R. Ganguly, R. Kinjo, *Chem. Eur. J.* **2016**, *22*, 9976–9985.
- [52] G. Baccolini, E. Mezzina, P. E. Todesco, E. Foresti, *J. Chem. Soc. Chem. Commun.* **1988**, 304–305.
- [53] G. Baccolini, E. Mezzina, P. E. Todesco, *J. Chem. Soc. Perkin Trans. 1* **1988**, 3281–3283.
- [54] G. Baccolini, C. A. Mesticchio, E. Mezzina, C. Rizzoli, P. Sgarabotto, *Heteroat. Chem.* **1993**, *4*, 319–322.
- [55] J. Abbenseth, O. P. E. Townrow, J. M. Goicoechea, *Angew. Chem. Int. Ed.* **2021**, *60*, 23625–23629.
- [56] J. I. van der Vlugt, *Top. Organomet. Chem.* **2021**, *68*, 135–179.
- [57] J. I. van der Vlugt, *Chem. Eur. J.* **2019**, *25*, 2651–2662.
- [58] O. R. Luca, R. H. Crabtree, *Chem. Soc. Rev.* **2013**, *42*, 1440–1459.
- [59] G. Zeng, S. Maeda, T. Taketsugu, S. Sakaki, *J. Am. Chem. Soc.* **2016**, *138*, 13481–13484.
- [60] D. Yang, P. Bao, Z. Yang, Z. Chen, S. Sakaki, S. Maeda, G. Zeng, *ChemCatChem* **2021**, *13*, 3925–3929.
- [61] Q. Zhu, R. Qiu, S. Dong, G. Zeng, J. Zhu, *Chem. Asian J.* **2021**, *16*, 2063–2067.
- [62] J. Underhill, E. S. Yang, T. Schmidt-Räntsch, W. K. Myers, J. M. Goicoechea, J. Abbenseth, *Chem. Eur. J.* **2023**, *29*, e202203266.
- [63] See Supporting Information for all experimental details, spectra and single crystal X-ray data. See Supporting Information for all experimental details. Deposition Numbers 2245882 (2), 2245883 (3^{me}),

- 2245884 (3^{IP}), 2245885 (4^{IP}), 2245886 (6), 2245887 (7-hex), 2245888 (8), 2245889 (9), 2245890 (10), 2245891 (11), 2245892 (12), 2245893 (14), 2245894 (15) and 2245895 (for 16) contains the supplementary crystallographic data for this paper. These data are provided free of charge by the joint Cambridge Crystallographic Data Centre and Fachinformationszentrum Karlsruhe Access Structures service.
- [64] K. M. Marczenko, J. A. Zurakowski, M. B. Kindervater, S. Jee, T. Hynes, N. Roberts, S. Park, U. Werner-Zwanziger, M. Lumsden, D. N. Langelaan, S. S. Chitnis, *Chem. Eur. J.* **2019**, *25*, 16414–16424.
- [65] S. E. Frazier, R. P. Nielsen, H. H. Sisler, *Inorg. Chem.* **1964**, *3*, 292–294.
- [66] S. F. Spangenberg, H. H. Sisler, *Inorg. Chem.* **1969**, *8*, 1006–1010.
- [67] J. C. Summers, H. H. Sisler, *Inorg. Chem.* **1970**, *9*, 862–869.
- [68] A. Schumann, F. Reiß, H. Jiao, J. Rabeah, J.-E. Siewert, I. Krummenacher, H. Braunschweig, C. Hering-Junghans, *Chem. Sci.* **2019**, *10*, 7859–7867.
- [69] J.-E. Siewert, A. Schumann, C. Hering-Junghans, *Dalton Trans.* **2021**, *50*, 15111–15117.
- [70] L. Falivene, Z. Cao, A. Petta, L. Serra, A. Poater, R. Oliva, V. Scarano, L. Cavallo, *Nat. Chem.* **2019**, *11*, 872–879.
- [71] S. Volodarsky, I. Malahov, D. Bawari, M. Diab, N. Malik, B. Tumanskii, R. Dobrovetsky, *Chem. Sci.* **2022**, *13*, 5957–5963.
- [72] A. Okuniewski, D. Rosiak, J. Chojnacki, B. Becker, *Polyhedron* **2015**, *90*, 47–57.
- [73] D. W. Allen, B. F. Taylor, *J. Chem. Soc. Dalton Trans.* **1982**, 51–54.
- [74] A. Sarbajna, V. S. V. S. N. Swamy, V. H. Gessner, *Chem. Sci.* **2021**, *12*, 2016–2024.
- [75] P. Pyykkö, *J. Phys. Chem. A* **2015**, *119*, 2326–2337.
- [76] L. Alig, M. Fritz, S. Schneider, *Chem. Rev.* **2019**, *119*, 2681–2751.
- [77] R. J. Somerville, J. Campos, *Eur. J. Inorg. Chem.* **2021**, 3488–3498.
- [78] B. Chatterjee, W.-C. Chang, S. Jena, C. Werlé, *ACS Catal.* **2020**, *10*, 14024–14055.
- [79] M. R. Elsby, R. T. Baker, *Chem. Soc. Rev.* **2020**, *49*, 8933–8987.
- [80] E. R. M. Habraken, A. R. Jupp, M. B. Brands, M. Nieger, A. W. Ehlers, J. C. Slootweg, *Eur. J. Inorg. Chem.* **2019**, 2436–2442.
- [81] T. Higashi, S. Kusumoto, K. Nozaki, *Chem. Rev.* **2019**, *119*, 10393–10402.
- [82] J. R. Khusnutdinova, D. Milstein, *Angew. Chem. Int. Ed.* **2015**, *54*, 12236–12273.
- [83] S. Yao, M. Brym, C. van Wüllen, M. Driess, *Angew. Chem. Int. Ed.* **2007**, *46*, 4159–4162.
- [84] T. Oishi, L. I. Lugo-Fuentes, Y. Jing, J. O. C. Jimenez-Halla, J. Barroso-Flores, M. Nakamoto, Y. Yamamoto, N. Tsunoi, R. Shang, *Chem. Commun.* **2021**, *12*, 15603–15608.
- [85] F. Dankert, M. Fischer, C. Hering-Junghans, *Dalton Trans.* **2022**, *51*, 11267–11276.
- [86] J. E. Griffiths, A. B. Burg, *J. Am. Chem. Soc.* **1960**, *82*, 1507–1508.
- [87] W. J. Bailey, R. B. Fox, *J. Org. Chem.* **1963**, *28*, 531–534.
- [88] W. J. Bailey, R. B. Fox, *J. Org. Chem.* **1964**, *29*, 1013–1017.
- [89] I. G. M. Campbell, I. D. R. Stevens, *Chem. Commun.* **1966**, 505–506.
- [90] B. Hoge, S. Neufeind, S. Hettel, W. Wiebe, C. Thösen, *J. Organomet. Chem.* **2005**, *690*, 2382–2387.
- [91] A. Christiansen, C. Li, M. Garland, D. Selent, R. Ludwig, A. Spannenberg, W. Baumann, R. Franke, A. Börner, *Eur. J. Org. Chem.* **2010**, 2733–2741.
- [92] B. G. Janesko, H. C. Fisher, M. J. Bridle, J.-L. Montchamp, *J. Org. Chem.* **2015**, *80*, 10025–10032.
- [93] A. Hubbard, T. Okazaki, K. K. Laali, *J. Org. Chem.* **2008**, *73*, 316–319.

Manuscript received: March 14, 2023

Accepted manuscript online: April 12, 2023

Version of record online: May 23, 2023